Spacer length dependent architectural diversity in bis-dipyrrin copper(II) complexes

Rajendra Prasad Paitandi, Roop Shikha Singh, Sujay Mukhopadhyay, Ashish Kumar and Daya Shankar Pandey*

Department of Chemistry, Institute of Science, Banaras Hindu University, Varanasi - 221005, India

---

Contents

Experimental Section

Characterization data of L1. Yield: 72% (3.51 g). Anal. Calc for $C_{32}H_{30}N_4O_2$: ESI-MS. (Calcd, found, *m/z*) 502.2369, 501.2256 $[M - \text{pyrrole} + Na + CH_3CN]^+$. ^1H NMR ($CDCl_3$, 300 MHz, δ ppm): 4.30 (s, 4H), 5.43 (s, 2H), 5.90 (s, 4H), 6.15 (d, J = 2.7 Hz, 4H), 6.69 (s, 4H), 6.89 (d, J = 8.4 Hz, 4H), 7.13 (d, J = 8.4 Hz, 4H), 7.93 (br, 4H). ^{13}C NMR ($CDCl_3$, 75 MHz, δ ppm): 38.4, 67.9, 106.6, 108.0, 113.6, 116.8, 117.0, 121.9, 128.1, 130.0, 131.8, 132.4, 155.7. IR (KBr pellets, cm^{-1}): 710, 729, 1029, 1050, 1091, 1251, 1291, 1396, 1452, 1492, 1561, 1598, 2872, 2944, 3374, 3408.

Characterization data of L2. Yield: 70% (3.61 g). Anal. Calc for $C_{33}H_{32}N_4O_2$: ESI-MS. (Calcd, found, *m/z*) 516.2525, 515.2642 $[M - \text{pyrrole} + Na + CH_3CN]^+$. ^1H NMR ($CDCl_3$, 300 MHz, δ ppm): δ 2.22 (s, 2H), 4.11 (s, 4H), 5.88 (s, 2H), 6.12 (s, 4H), 6.24 (s, 4H), 6.69 (s, 4H), 6.82 (d, J = 7.8 Hz, 4H), 7.08 (d, J = 7.5 Hz, 4H), 7.89 (br, 4H). ^{13}C NMR ($CDCl_3$, 75MHz, δ ppm): 38.3, 65.1, 106.5, 108.0, 112.4, 116.6, 121.2, 128.1, 129.6, 130.9, 132.4, 155.9. IR (KBr pellets, cm^{-1}): 710, 729, 1028, 1049, 1091, 1250, 1291, 1397, 1451, 1490, 1560, 1596, 2872, 2942, 3376, 3410.

Characterization data of L3. Yield: 69% (3.65 g). Anal. Calc for $C_{34}H_{34}N_4O_2$: ESI-MS. (Calcd, found, *m/z*) 530.2682, 529.2599 $[M - \text{pyrrole} + Na + CH_3CN]^+$. ^1H NMR ($CDCl_3$, 300 MHz, δ ppm): 1.80 (s, 4H), 3.94 (s, 4H), 5.42 (s, 2H), 5.90 (s, 4H), 6.14 (d, J = 2.7 Hz, 4H), 6.68 (s, 4H), 6.82 (d, J = 8.4 Hz, 4H), 7.18 (d, J = 8.1 Hz, 4H), 7.90 (br, 4H). ^{13}C NMR ($CDCl_3$, 75 MHz, δ ppm): 25.9, 43.1, 67.4, 106.9, 108.3, 114.5, 117.0, 129.3, 132.8, 134.1, 157.9. IR (KBr pellets, cm^{-1}): 710, 728, 1029, 1051, 1091, 1251, 1290, 1397, 1450, 1492, 1560, 1596, 2871, 2940, 3375, 3408.

Characterization data of L3′. Yield: 69% (3.65 g). Anal. Calc for $C_{34}H_{34}N_4O_2$: ^1H NMR ($CDCl_3$, 300 MHz, δ ppm): 1.96 (s, 4H), 4.01 (s, 4H), 5.42 (s, 2H), 5.90 (s, 4H), 6.15 (d, J = 2.7 Hz, 4H), 6.68 (s, 4H), 6.82 (d, J = 8.4 Hz, 4H), 7.13 (d, J = 8.1 Hz, 4H), 7.91 (br, 4H). ^{13}C NMR ($CDCl_3$, 75 MHz, δ ppm): 25.9, 29.6, 67.4, 106.9, 108.3, 114.5, 129.3, 132.8, 134.1, 157.9. IR (KBr pellets, cm^{-1}): 709, 743, 841, 1010, 1087, 1090, 1177, 1245, 1300, 1422, 1475, 1513, 1557, 1610, 2868, 2944, 3361, 3431.

Characterization data of L4. Yield, 65% (3.53 g). Anal. Calc for $C_{35}H_{36}N_4O_2$: ESI-MS. (Calcd, found, *m/z*) 544.2348, 543.2955 $[M - \text{pyrrole} + Na + CH_3CN]^+$, 567.2939 $[M + Na]^+$, 583.2836 $[M + K]^+$. ^1H NMR ($CDCl_3$, 300 MHz, δ ppm): 1.20 (m, 2H), 2.22 (t, J = 5.4 Hz, 4H), 4.12 (t, J = 6.3 Hz, 4H), 5.39 (s, 2H), 5.88 (s, 4H), 6.13 (s, 4H), 6.65 (s, 4H), 6.84 (d, J = 7.2 Hz, 4H), 7.09 (d, J = 7.5 Hz, 4H), 7.87 (br, 4H). ^{13}C NMR ($CDCl_3$, 75 MHz, δ ppm):

25.9, 29.2, 43.1, 67.9, 107.0, 108.4, 114.5, 117.0, 129.3, 132.8. IR (KBr pellets, cm^{-1}): 710, 729, 1029, 1050, 1091, 1251, 1291, 1396, 1452, 1492, 1561, 1598, 2868, 2940, 3374, 3408.

Characterization data of L5. Yield, 62% (3.45 g). Anal. Calc for $C_{36}H_{38}N_4O_2$: ESI-MS. (Calcd, found, *m/z*) 558.2995, 557.2716 $[M - pyrrole + Na + CH_3CN]^+$, 581.2697 $[M + Na]^+$, 597.2597 $[M + K]^+$. ^1H NMR ($CDCl_3$, 500 MHz, δ ppm): 1.46 (t, J = 6.5 Hz, 4H), 1.73 (t, J = 6.5 Hz, 4H), 3.87 (t, J = 7.5 Hz, 4H), 5.34 (s, 2H), 5.83 (s, 4H), 6.08 (q, 4H), 6.61 (d, J = 1.5 Hz, 4H), 6.76 (d, J = 8.5 Hz, 4H), 7.04 (d, J = 8.5 Hz, 4H), 7.85 (br, 4H). ^{13}C NMR ($CDCl_3$, 125 MHz, δ ppm): 25.9, 29.2, 43.2, 67.9, 107.0, 108.4, 116.4, 117.1, 129.4, 132.9, 134.1, 158.1. IR (KBr pellets, cm^{-1}): 710, 729, 1027, 1049, 1090, 1249, 1290, 1393, 1451, 1490, 1561, 1597, 2865, 2938, 3374, 3406.

Characterization data of L6. Yield, 63% (3.60 g). Anal. Calc for $C_{37}H_{40}N_4O_2$: ESI-MS. (Calcd, found, *m/z*) 572.3151, 595.3213 $[M + Na]^+$. ^1H NMR ($CDCl_3$, 300 MHz, δ ppm): 0.88 (m, 2H), 1.27 (s, 4H), 1.77 (s, 4H), 3.92 (s, 4H), 5.38 (s, 2H), 5.89 (s, 4H), 6.13 (s, 4H), 6.65 (s, 4H), 6.81 (d, J = 7.8 Hz, 4H), 7.05 (s, 4H), 7.87 (br, 4H). ^{13}C NMR ($CDCl_3$, 75 MHz, δ ppm): 25.9, 29.0, 43.0, 67.8, 106.9, 108.3, 108.6, 114.5, 117.0, 129.3, 132.8, 133.9, 158.0. IR (KBr pellets, cm^{-1}): 711, 729, 1029, 1050, 1091, 1247, 1290, 1392, 1452, 1492, 1561, 1598, 2863, 2936, 3374, 3408.

Characterization data of L7. Yield, 62% (3.63 g). Anal. Calc for $C_{38}H_{42}N_4O_2$: ESI-MS. (Calcd, found, *m/z*) 586.3308, 585.3641 $[M - pyrrole + Na + CH_3CN]^+$, 609.3632 $[M + Na]^+$, 625.3435 $[M + K]^{+\cdot}$ ^1H NMR ($CDCl_3$, 300 MHz, δ ppm): 1.40 –1.53 (s, 8H), 1.76 (t, J = 1.5 Hz, 4H), 3.92 (t, J = 6.6 Hz, 4H), 5.41 (s, 2H), 5.90 (s, 4H), 6.13 (d, J = 2.7 Hz, 4H), 6.67 (s, 4H), 6.82 (d, J = 8.7 Hz, 4H), 7.09 (d, J = 8.4 Hz, 4H), 7.90 (br, 4H). ^{13}C NMR ($CDCl_3$, 75 MHz, δ ppm): 25.9, 29.2, 43.1, 67.9, 107.0, 108.4, 114.5, 117.0, 129.3, 132.8. IR (KBr pellets, cm^{-1}): 710, 1029, 1050, 1091, 1246, 1291, 1391, 1452, 1492, 1561, 1598, 2862, 2933, 3409.

Characterization data of L8. Yield, 61% (3.66 g). Anal. Calc for $C_{39}H_{44}N_4O_2$: ESI-MS. (Calcd, found, *m/z*) 600.3464, 599.3437 $[M - pyrrole + Na + CH_3CN]^+$, 623.3413 $[M + Na]^+$, 639.3332 $[M + K]^+$. ^1H NMR ($CDCl_3$, 300 MHz, δ ppm): 1.34 (s, 10H), 1.75 (s, 4H), 3.91 (s, 4H), 5.36 (s, 2H,), 5.87 (s, 4H), 6.12 (s, 4H), 6.63 (s, 4H), 6.80 (d, J = 7.8 Hz, 4H), 7.07 (d, J = 7.2 Hz, 4H), 7.89 (br, 4H). ^{13}C NMR ($CDCl_3$, 75 MHz, δ ppm): 26.0, 29.2, 43.0, 68.0, 106.9, 108.3, 114.5, 117.0, 129.3, 132.9, 133.9, 158.0. IR (KBr pellets, cm^{-1}): 714, 1028, 1049, 1090, 1244, 1290, 1390, 1451, 1491, 1560, 1596, 2860, 2930, 3373, 3410.

Characterization data of L9. Yield, 65% (3.99 g). Anal. Calc for $C_{40}H_{46}N_4O_2$: ESI-MS. (Calcd, found, *m/z*) 614.3621, 613.3528 $[M - \text{pyrrole} + Na + CH_3CN]^+$. ^1H NMR ($CDCl_3$, 500 MHz, δ ppm): 1.22 (s, 12H), 1.70 (m, 4H), 3.87 (t, J = 6.5 Hz, 4H), 5.36 (s, 2H), 5.85 (s, 4H), 6.09 (t, J = 2.5 Hz, 4H), 6.63 (t, J = 2.5 Hz, 4H), 6.78 (t, J = 8.5 Hz, 4H), 7.05 (d, J = 8.5 Hz, 4H), 7.86 (br, 4H). ^{13}C NMR ($CDCl_3$, 125 MHz, δ ppm): 26.0, 29.2, 35.0, 43.0, 68.0, 106.9, 108.0, 108.3, 114.5, 117.0, 128.4, 129.3, 132.8. IR (KBr pellets, cm^{-1}): 715, 753, 1025, 1048, 1091, 1243, 1288, 1389, 1452, 1490, 1561, 1597, 2858, 2930, 3414.

Characterization data of 1. Yield 40% (0.164 g). Anal. Calc for $C_{42}H_{38}N_4O_6Cu_2$: ESI-MS. (Calcd, found, *m/z*) 845.1281, 845.1301 $[M + {}^{65}Cu + Na]^+$, 861.1046 $[M + {}^{65}Cu + K]^+$. IR (KBr pellets, cm^{-1}): 725, 890, 997, 1023, 1248, 1339, 1377, 1445, 1489, 1548, 1580, 2854, 2924.

Characterization data of 2. Yield 38% (0.158 g). Anal. Calc for $C_{43}H_{40}N_4O_6Cu_2$: ESI-MS. (Calcd, found, *m/z*) 859.1438, 859.1412 $[M + {}^{65}Cu + Na]^+$. IR (KBr pellets, cm^{-1}): 725, 890, 997, 1023, 1248, 1339, 1377, 1445, 1489, 1548, 1580, 2854, 2924.

Characterization data of 3. Yield 37% (0.157 g). Anal. Calc for $C_{44}H_{42}N_4O_6Cu_2$: ESI-MS. (Calcd, found, *m/z*) 873.1594, 873.1474 $[M + {}^{65}Cu + Na]^+$. IR (KBr pellets, cm^{-1}): 720, 832, 890, 996, 1034, 1245, 1334, 1375, 1445, 1490, 1549, 1580, 2852, 2925.

Characterization data of 3′. Yield 37% (0.157 g). Anal. Calc for $C_{44}H_{42}N_4O_6Cu_2$: ESI-MS. (Calcd, found, *m/z*) 873.1594, 873.1443 $[M + {}^{65}Cu + Na]^+$. IR (KBr pellets, cm^{-1}): 715, 734, 822, 890, 996, 1025, 1175, 1243, 1334, 1375, 1404, 1450, 1489, 1518, 1542, 1585, 1608, 2852, 2924.

Characterization data of 3″. Yield 42% (0.196 g). Anal. Calc for $C_{44}H_{48}N_6O_2S_4Ni_2$: ESI-MS. (Calcd, found, *m/z*) 961.1483, 961.1282 $[M + 2H + Na]^+$. ^1H NMR ($CDCl_3$, 300 MHz, δ ppm): 1.23 (s, 6H), 1.91 (s, 4H), 3. 75(s, 4H), 5.49 (s, 4H), 6.14 (d, J = 2.7Hz, 4H), 6.44 (d, J = 3.3Hz, 4H), 6.92 (d, J = 8.4Hz, 4H), 6.99 (d, J = 8.1Hz, 4H), 7.16–7.38 (m, 14H). ^{13}C NMR ($CDCl_3$, 75 MHz, δ ppm): 25.2, 25.4, 29.6, 68.0, 101.5, 112.7, 116.4, 119.4, 126.6, 129.7, 131.8, 134.9, 141.7, 147.4, 156.8, 186.8. IR (KBr pellets, cm^{-1}): 721, 988, 1030, 1506, 1530, 1586, 2854, 2923.

Characterization data of 4. Yield 35% (0.150 g). Anal. Calc for $C_{45}H_{44}N_4O_6Cu_2$: ESI-MS. (Calcd, found, *m/z*) 763.1407, 763.5030 $[M - acac]^+$. IR (KBr pellets, cm^{-1}): 721, 832, 890, 996, 1034, 1245, 1335, 1376, 1444, 1489, 1550, 1581, 2853, 2924.

Characterization data of 5. Yield 20% (0.088 g). Anal. Calc for $C_{46}H_{46}N_4O_6Cu_2$: ESI-MS. (Calcd, found, *m/z*) 901.1907, 901.1893 $[M + {}^{65}Cu + Na]^+$, 917.1637 $[M + {}^{65}Cu + K]^+$.

IR (KBr pellets, cm^{-1}): 720, 832, 889, 997, 1034, 1245, 1335, 1375, 1445, 1489, 1550, 1581, 2854, 2924.

Characterization data of 6. Yield 30% (0.094 g). Anal. Calc for $C_{37}H_{34}N_4O_2Cu$: ESI-MS. (Calcd, found, *m/z*) 630.2156, 630.2048 $[M + H]^+$. IR (KBr pellets, cm^{-1}): 727, 775, 890, 996, 1021, 1035, 1246, 1338, 1374, 1445, 1552, 2924.

Characterization data of 7. Yield 35% (0.112 g). Anal. Calc for $C_{38}H_{36}N_4O_2Cu$: ESI-MS. (Calcd, found, *m/z*) 644.2213, 644.2214 $[M + H]^+$. IR (KBr pellets, cm^{-1}): 727, 774, 889, 997, 1021, 1035, 1247, 1338, 1374, 1447, 1552, 2924.

Characterization data of 8. Yield 34% (0.111 g). Anal. Calc for $C_{39}H_{38}N_4O_2Cu$: ESI-MS. (Calcd, found, *m/z*) 658.2369, 658.2349 $[M + H]^+$. IR (KBr pellets, cm^{-1}): 727, 775, 890, 996, 1021, 1035, 1246, 1338, 1374, 1445, 1552, 2924.

Characterization data of 9. Yield 34% (0.111 g). Anal. Calc for $C_{40}H_{40}N_4O_2Cu$: ESI-MS. (Calcd, found, *m/z*) 694.2345, 694.2331 $[M + Na]^+$. IR (KBr pellets, cm^{-1}): 725, 773, 889, 997, 1034, 1246, 1336, 1375, 1446, 1553, 2852, 2924.

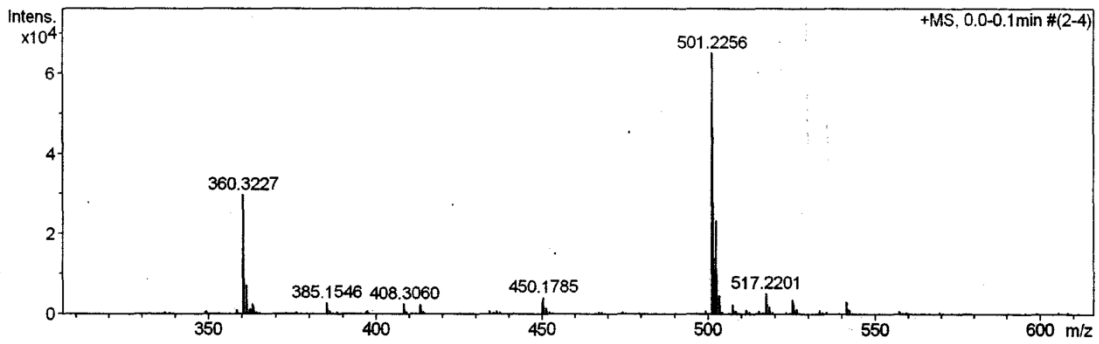

Fig. S1 Mass spectra of **L1**.

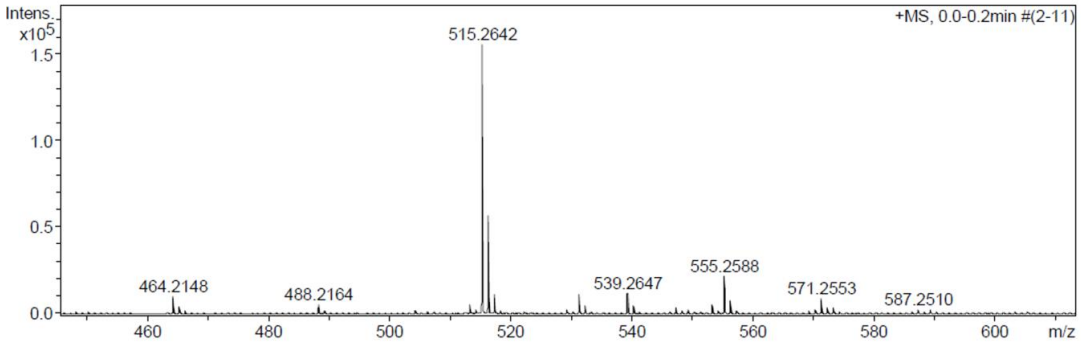

Fig. S2 Mass spectra of **L2**.

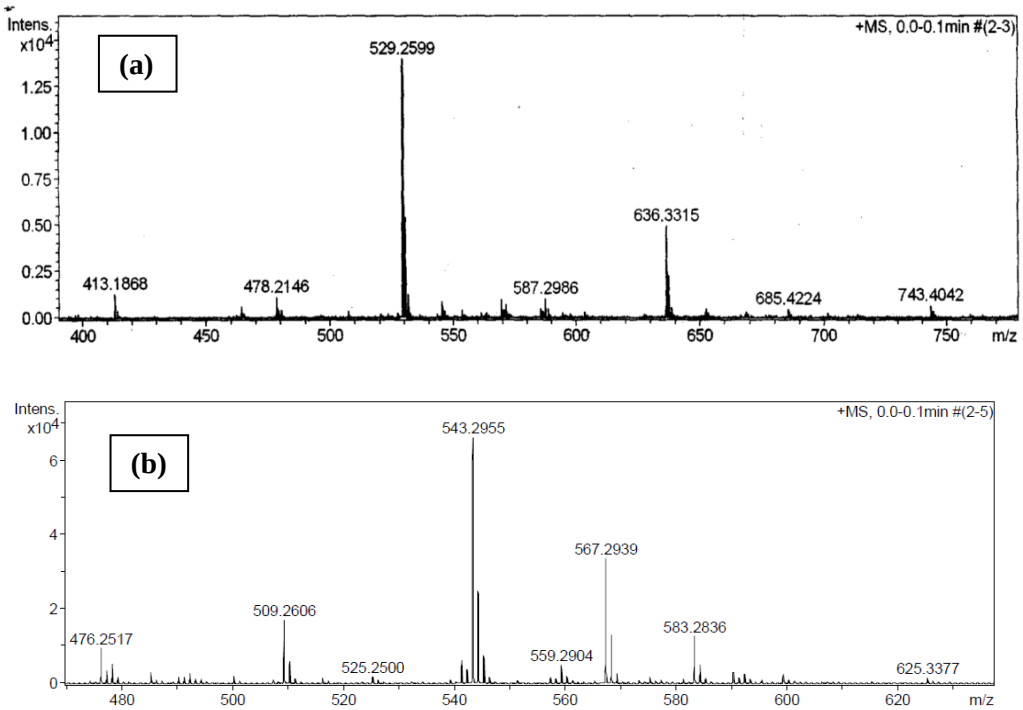

Fig. S3 Mass spectra of **L3** (a) and **L3′** (b).

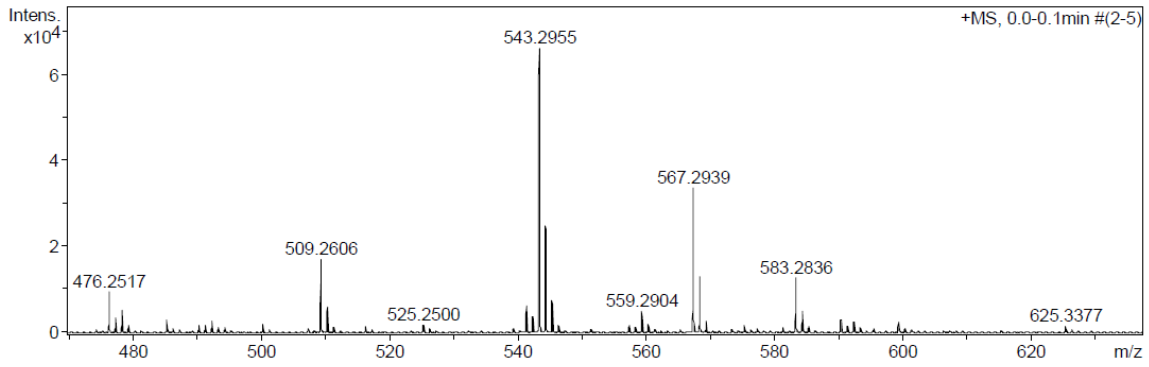

Fig. S4 Mass spectra of **L4**.

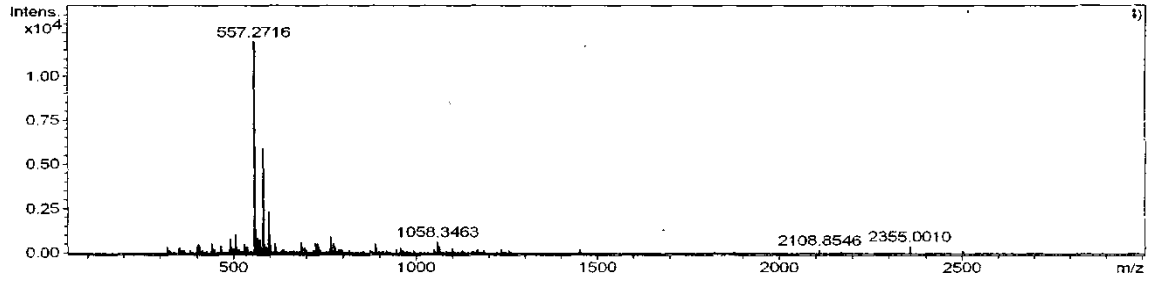

Fig. S5 Mass spectra of **L5**.

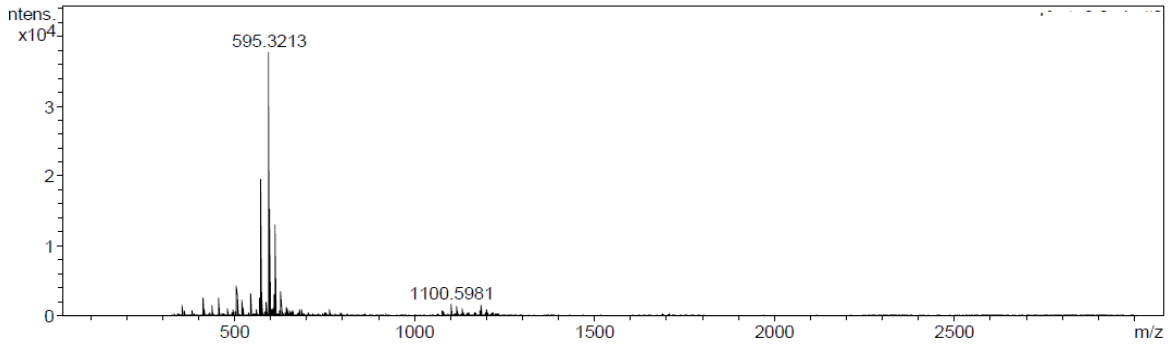

Fig. S6 Mass spectra of **L6**.

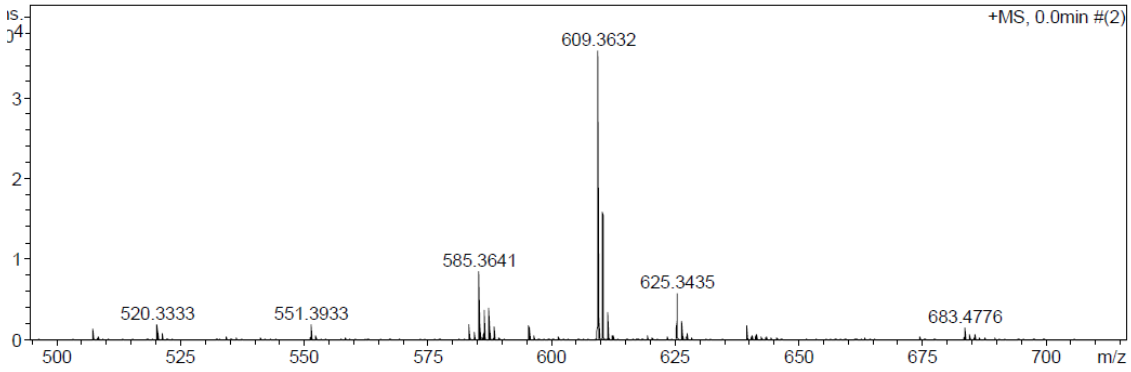

Fig. S7 Mass spectra of **L7**.

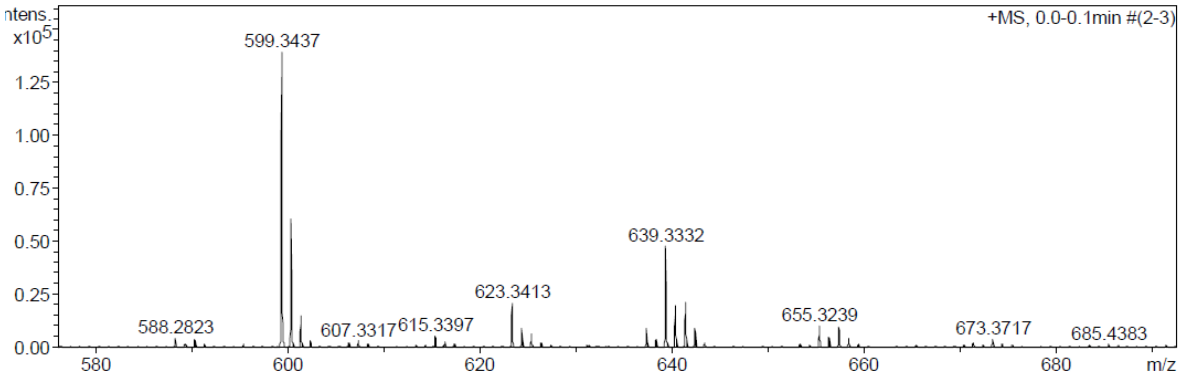

Fig. S8 Mass spectra of **L8**.

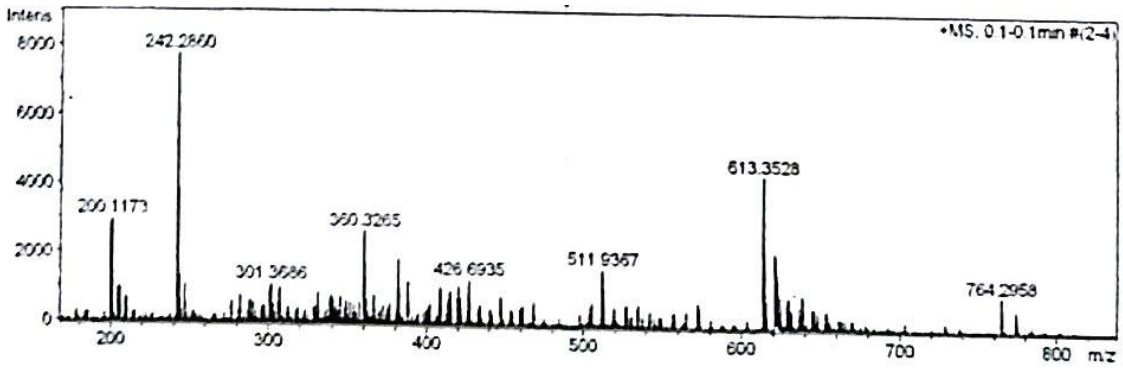

Fig. S9 Mass spectra of **L9**.

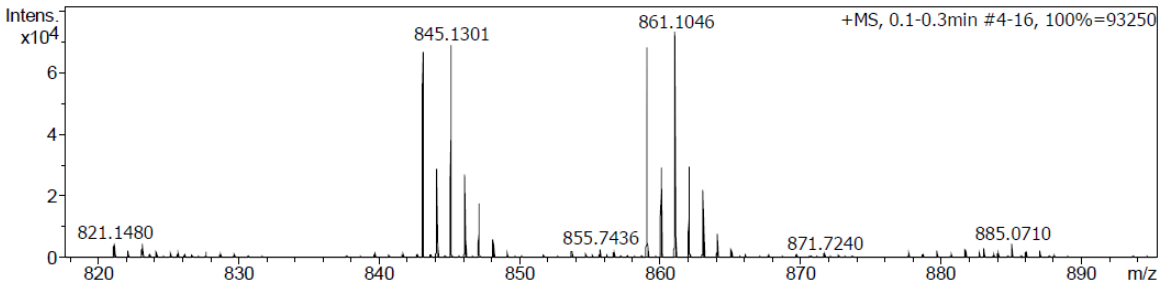

Fig. S10 Mass spectra of complex **1**.

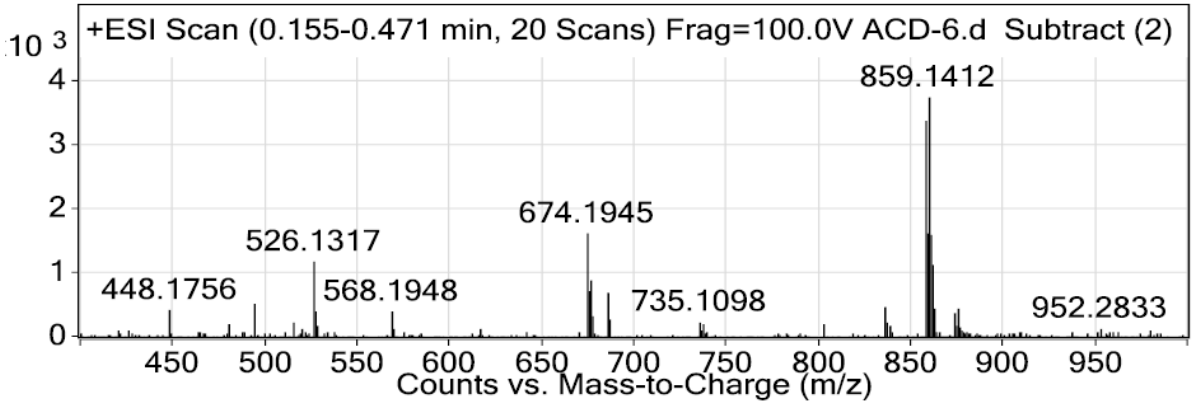

Fig. S11 Mass spectra of complex **2**.

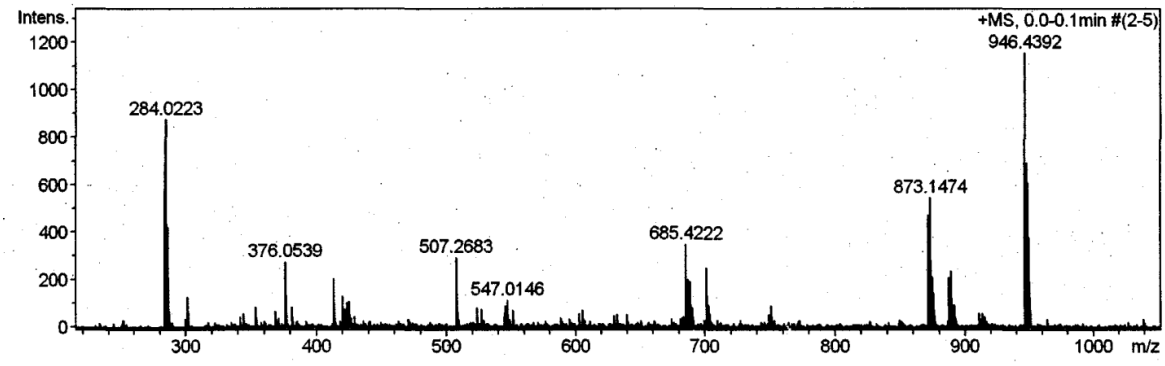

Fig. S12 Mass spectra of complex **3**.

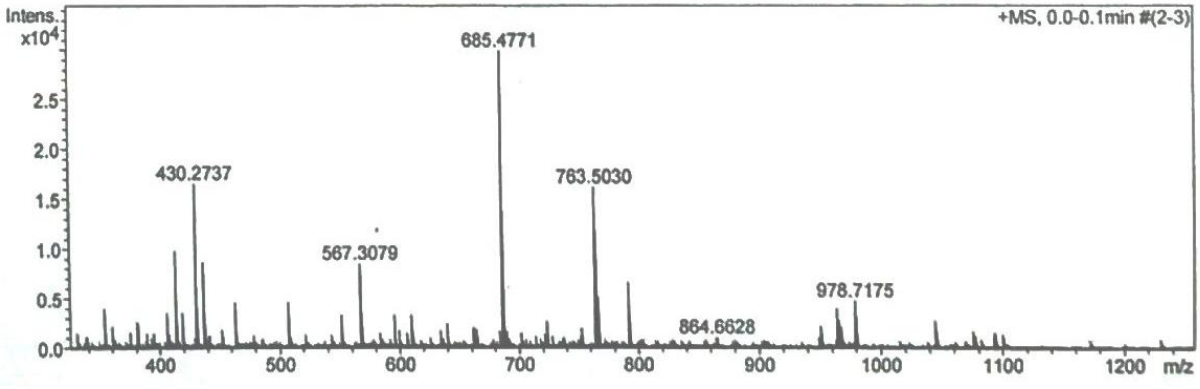

Fig. S13 Mass spectra of complex **4**.

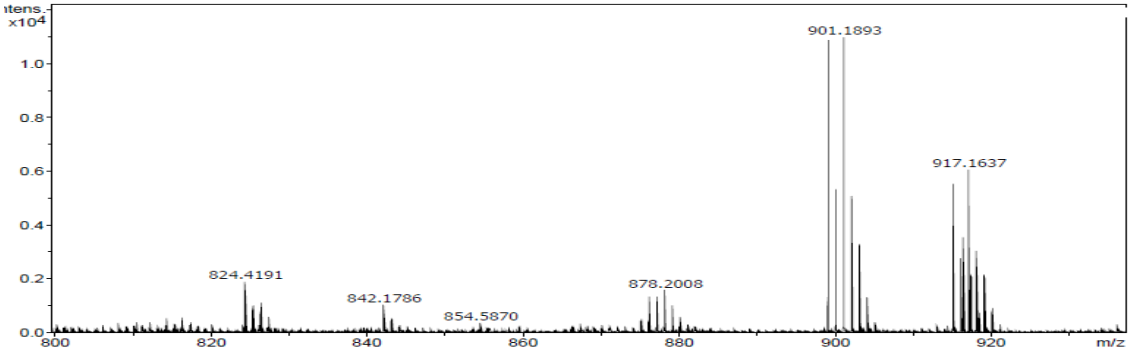

Fig. S14 Mass spectra of complex **5**.

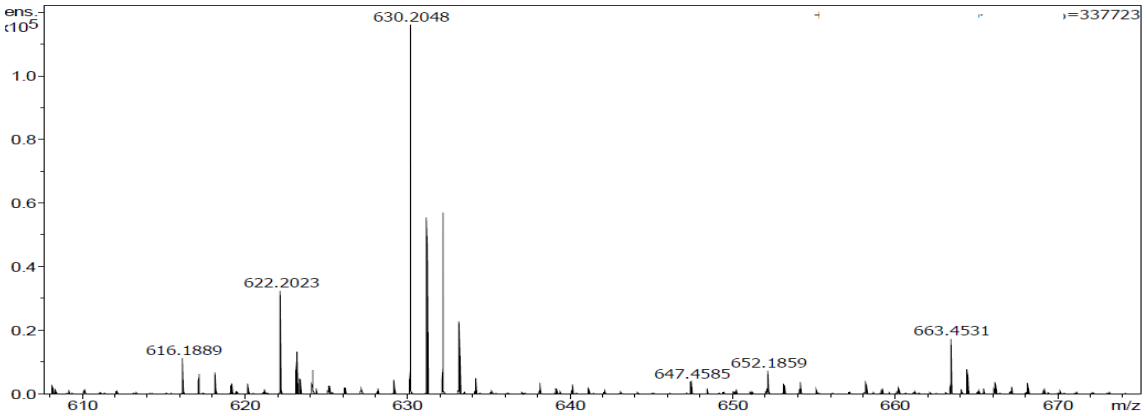

Fig. S15 Mass spectra of complex **6**.

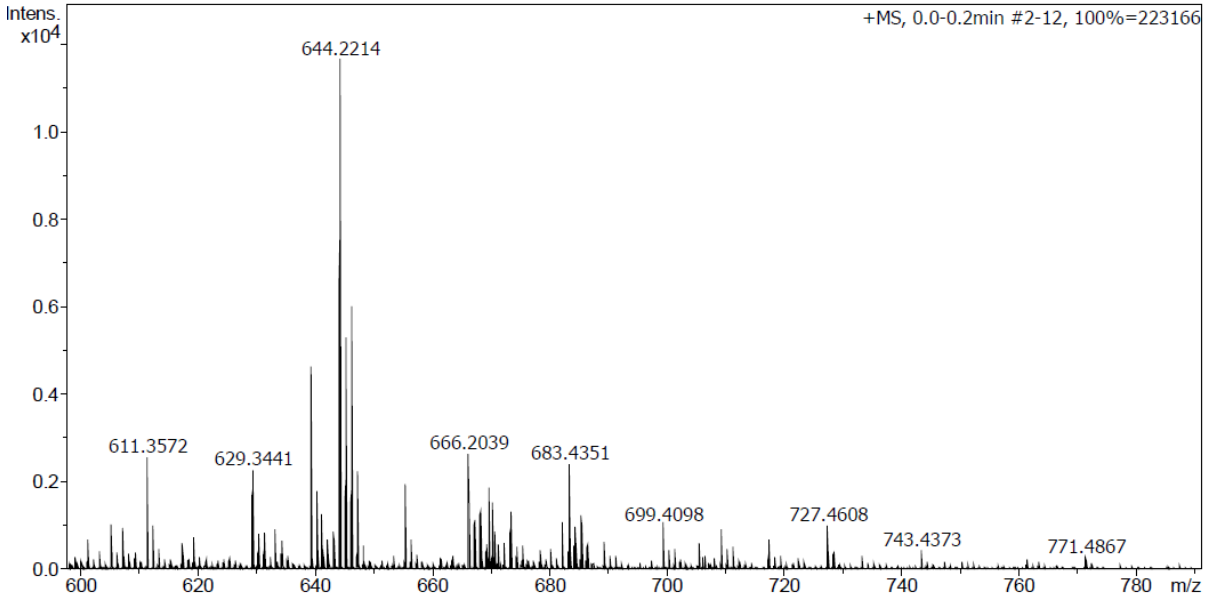

Fig. S16 Mass spectra of complex **7**.

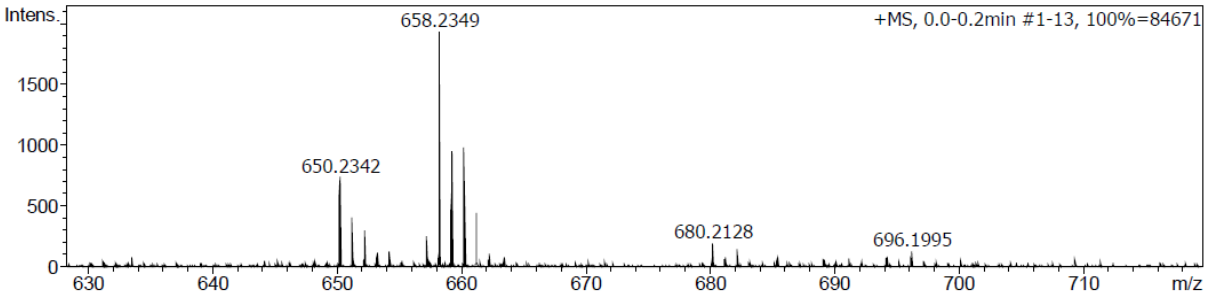

Fig. S17 Mass spectra of complex **8**.

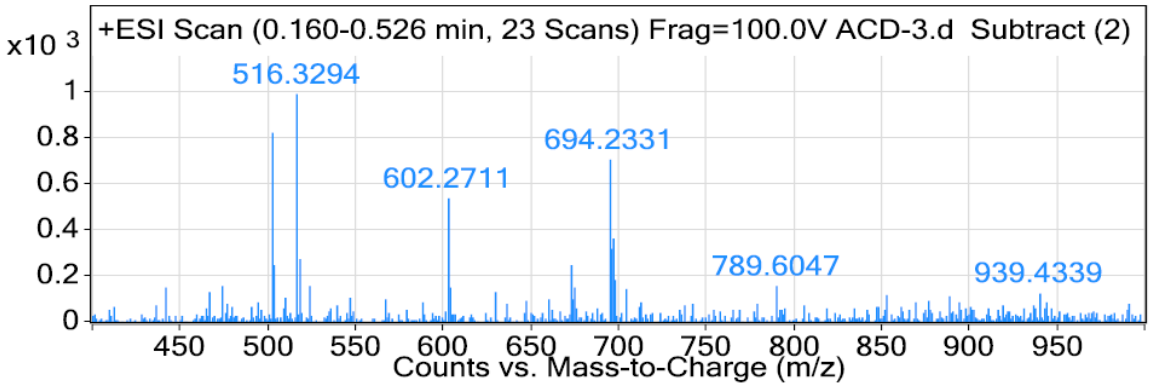

Fig. S18 Mass spectra of complex **9**.

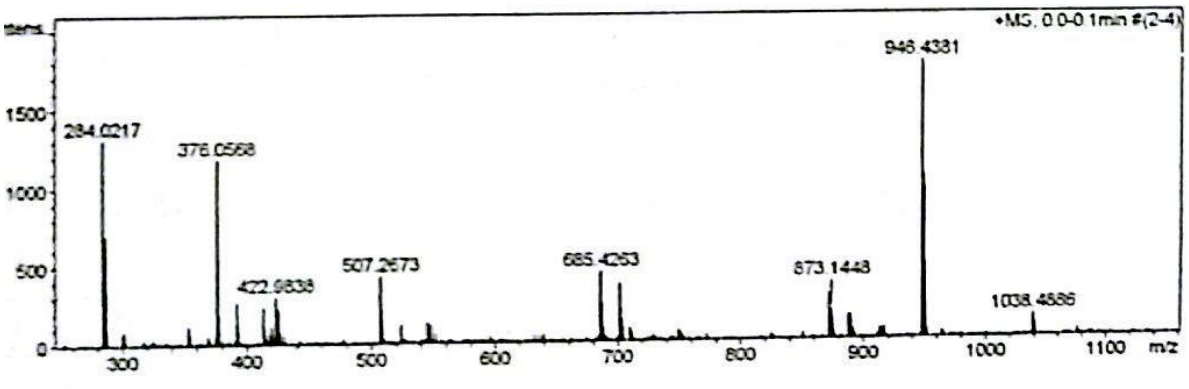

Fig. S19 Mass spectra of complex **3′**.

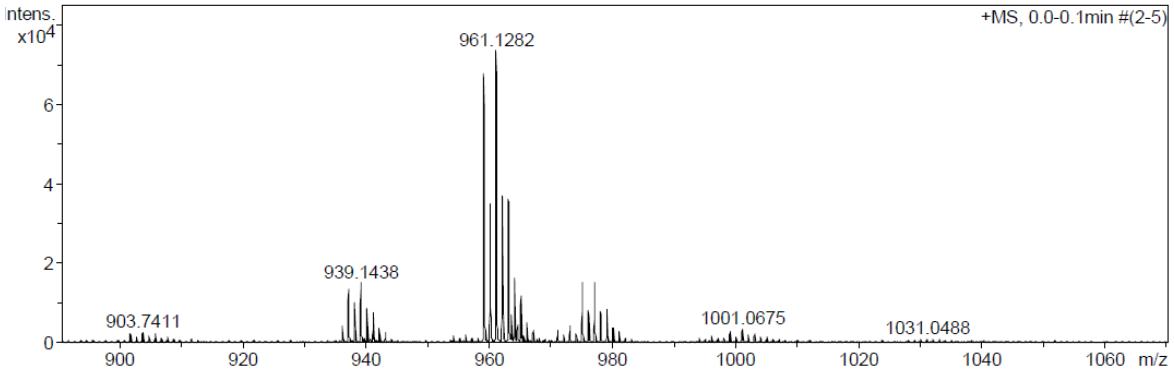

Fig. S20 Mass spectra of complex **3″**.

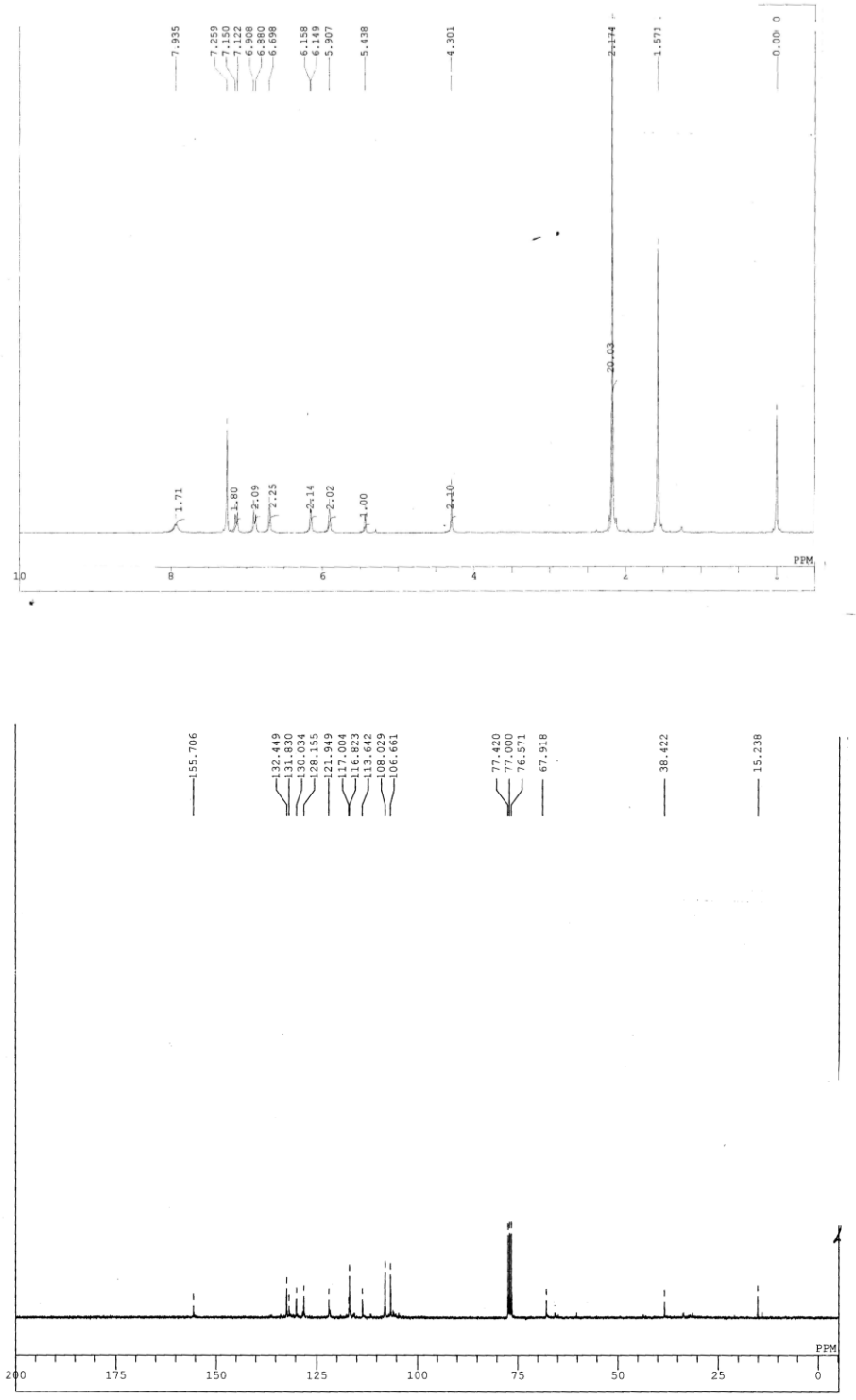

Fig. S21 ^{1}H (top) and ^{13}C NMR (bottom) spectra of **L1** in $CDCl_3$.

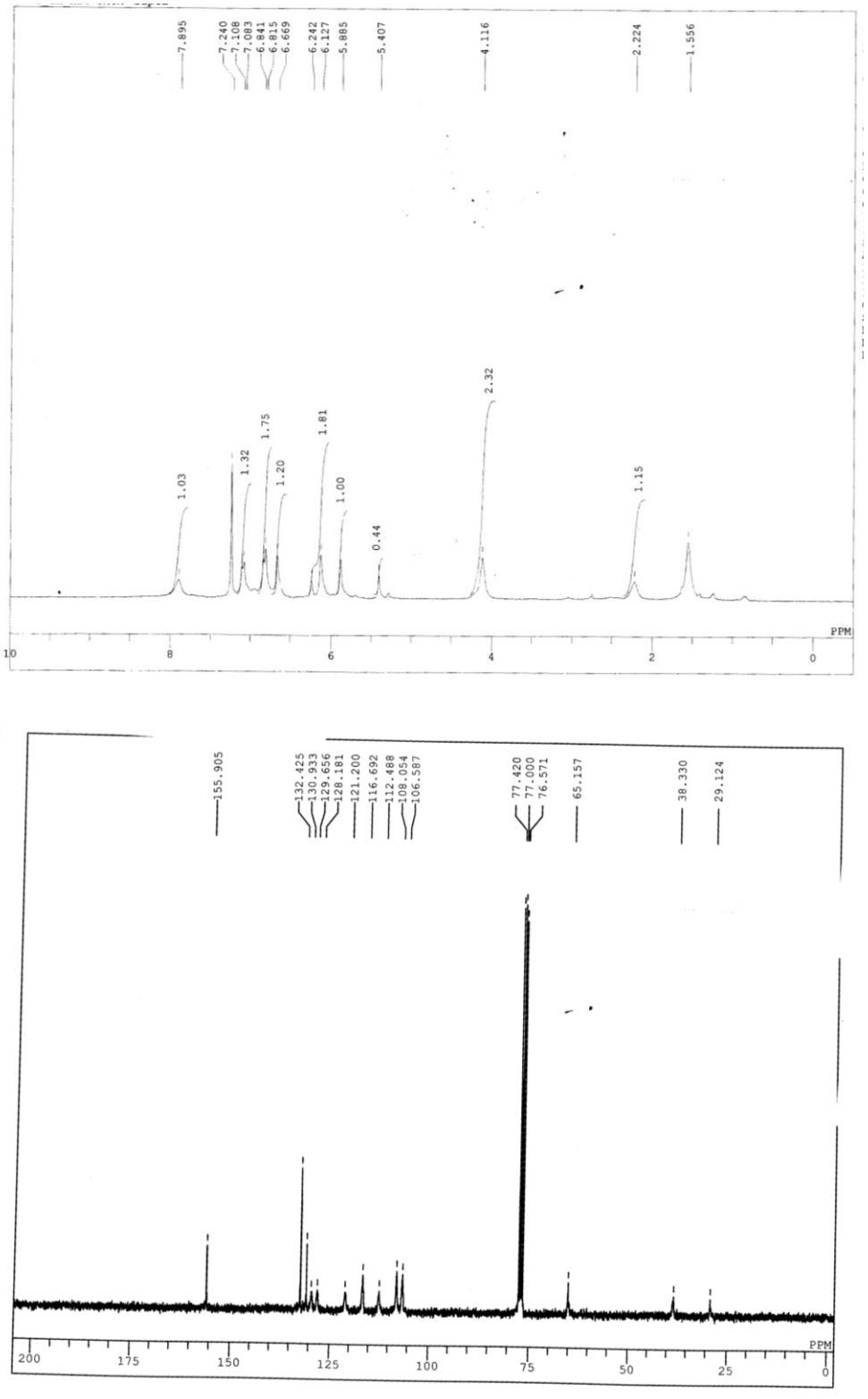

Fig. S22 ^{1}H (top) and ^{13}C NMR (bottom) spectra of **L2** in $CDCl_3$.

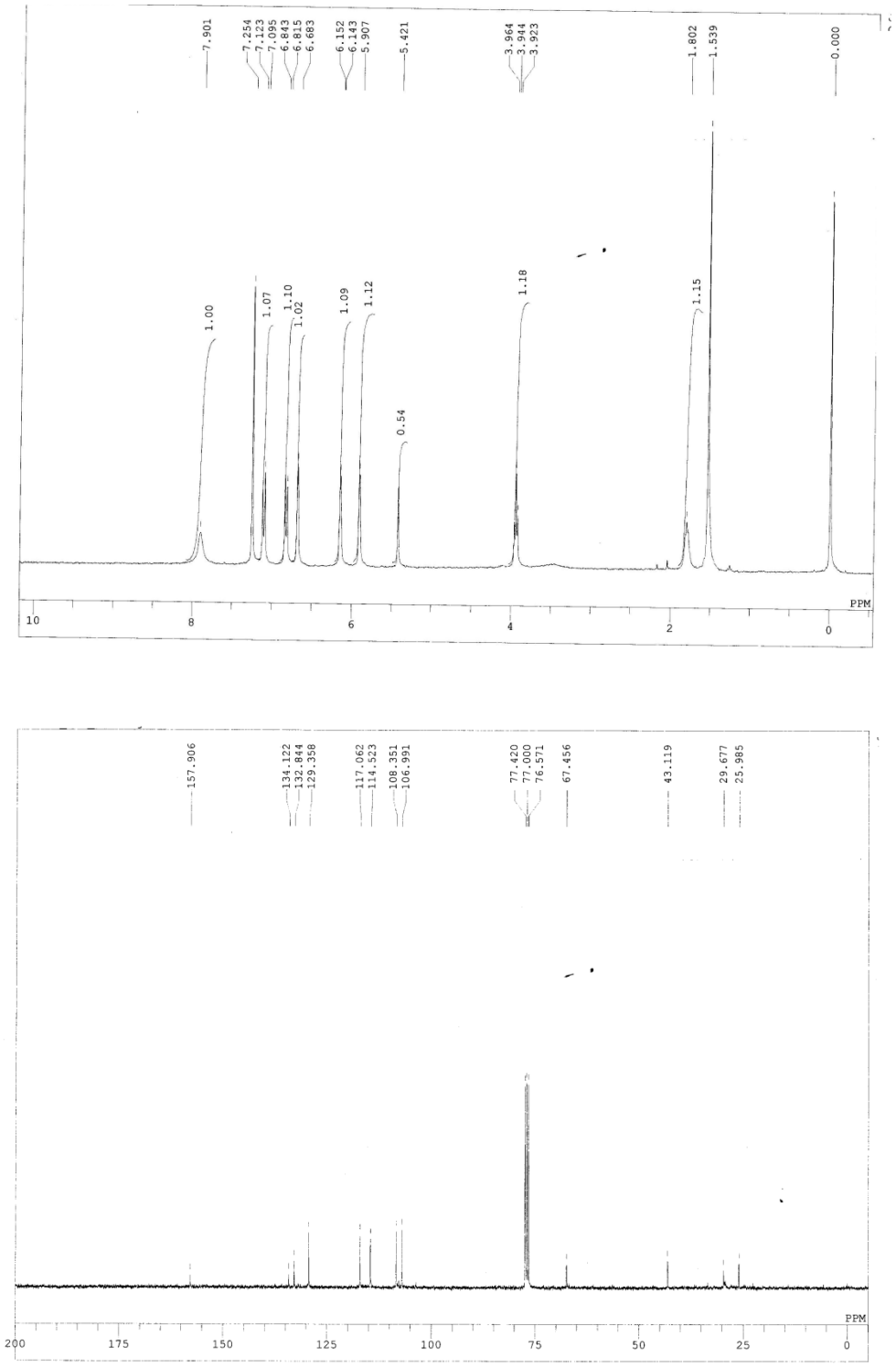

Fig. S23 ^{1}H (top) and ^{13}C NMR (bottom) spectra of **L3** in $CDCl_3$.

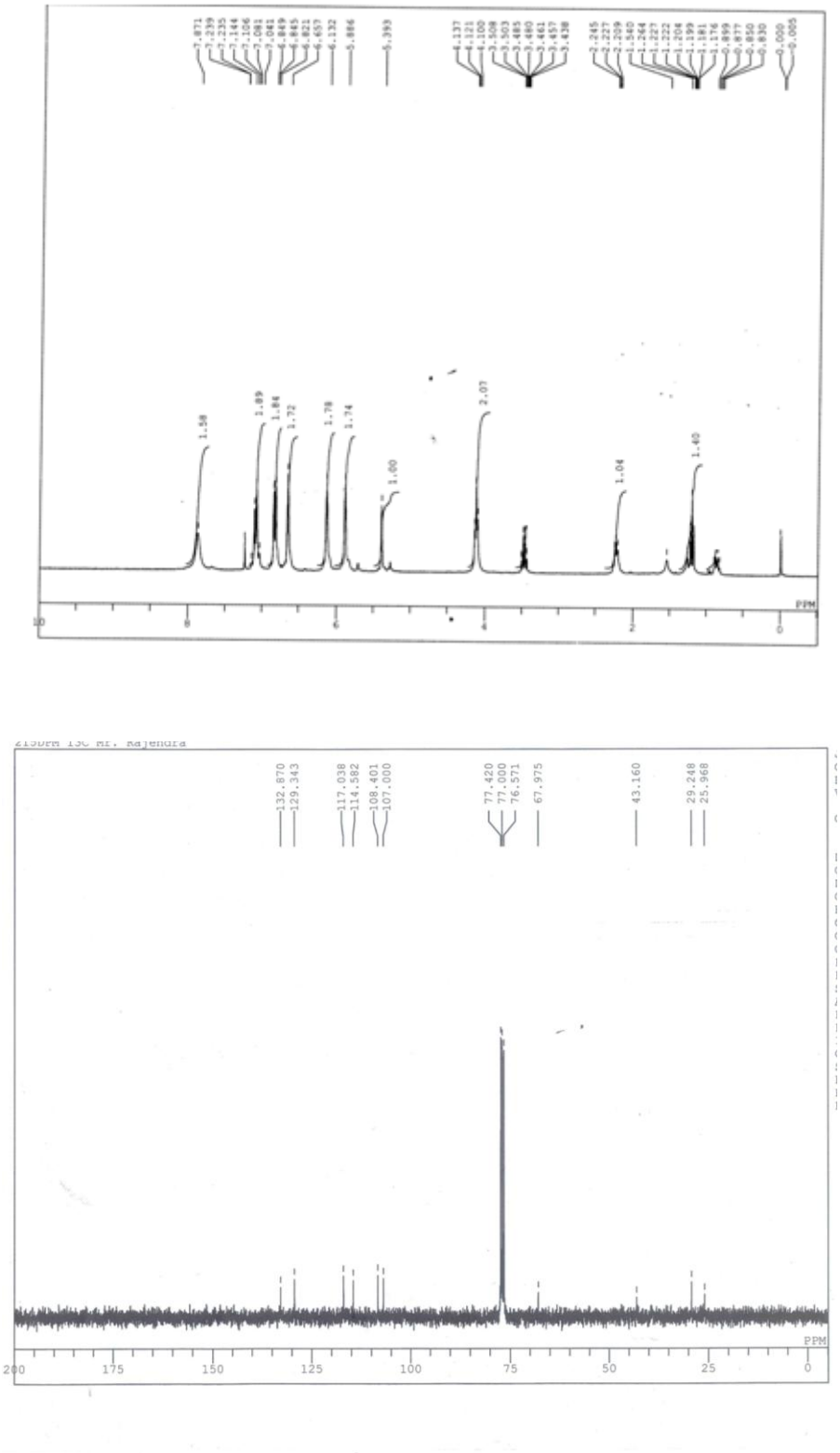

Fig. S24 ^{1}H (top) and ^{13}C NMR (bottom) spectra of **L4** in $CDCl_3$.

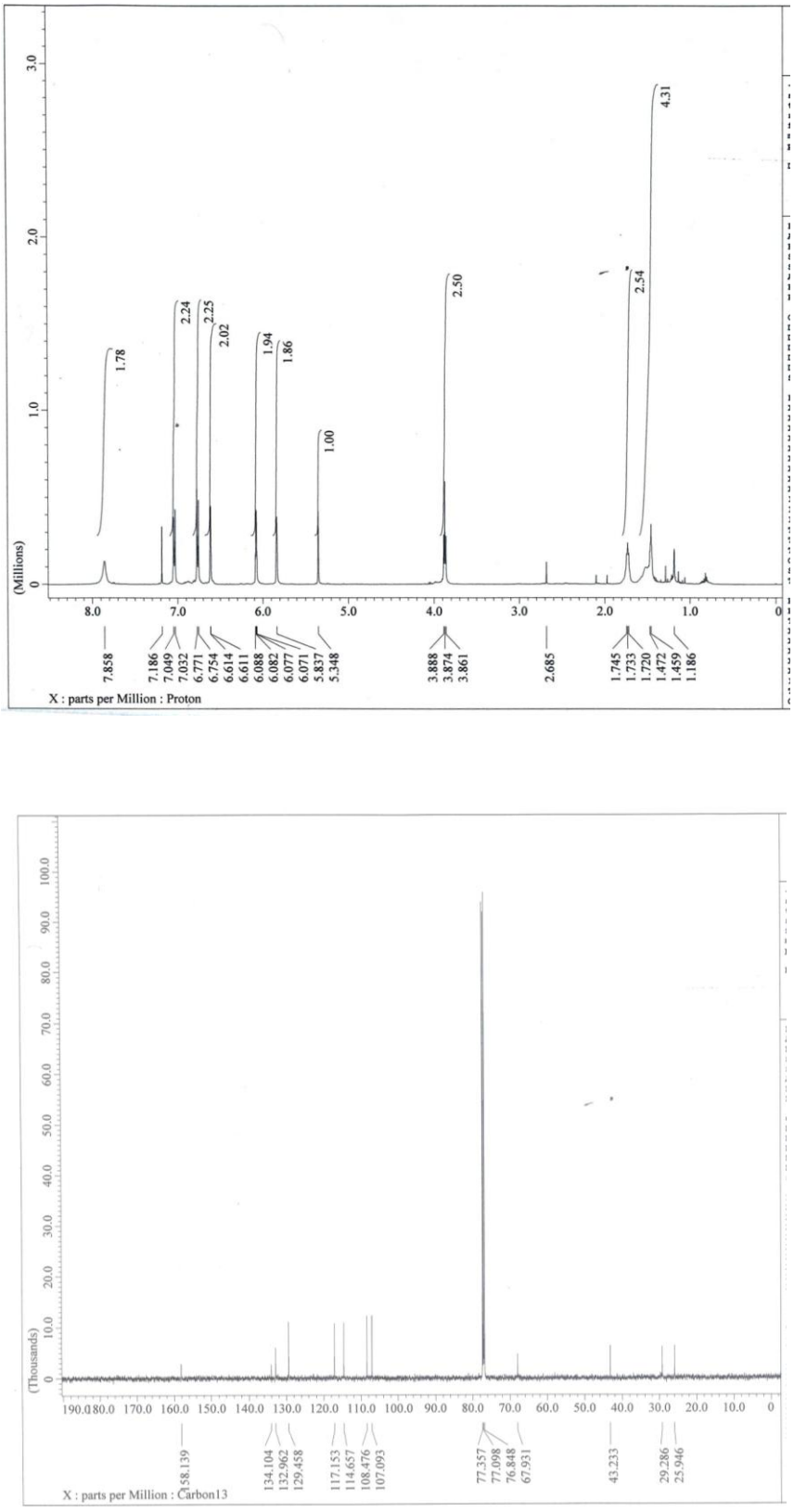

Fig. S25 ^{1}H (top) and ^{13}C NMR (bottom) spectra of **L5** in $CDCl_3$.

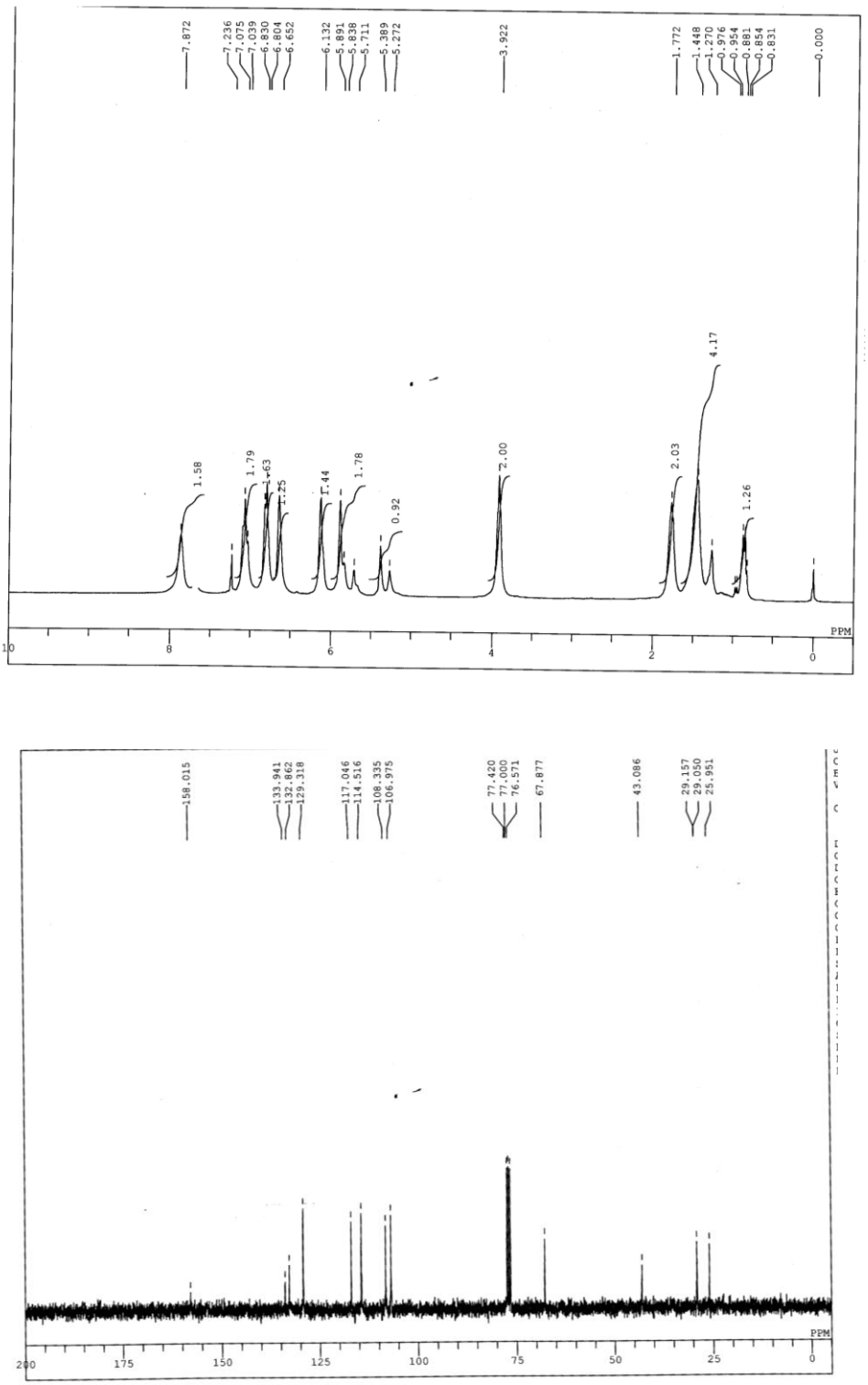

Fig. S26 ^{1}H (top) and ^{13}C NMR (bottom) spectra of **L6** in $CDCl_3$.

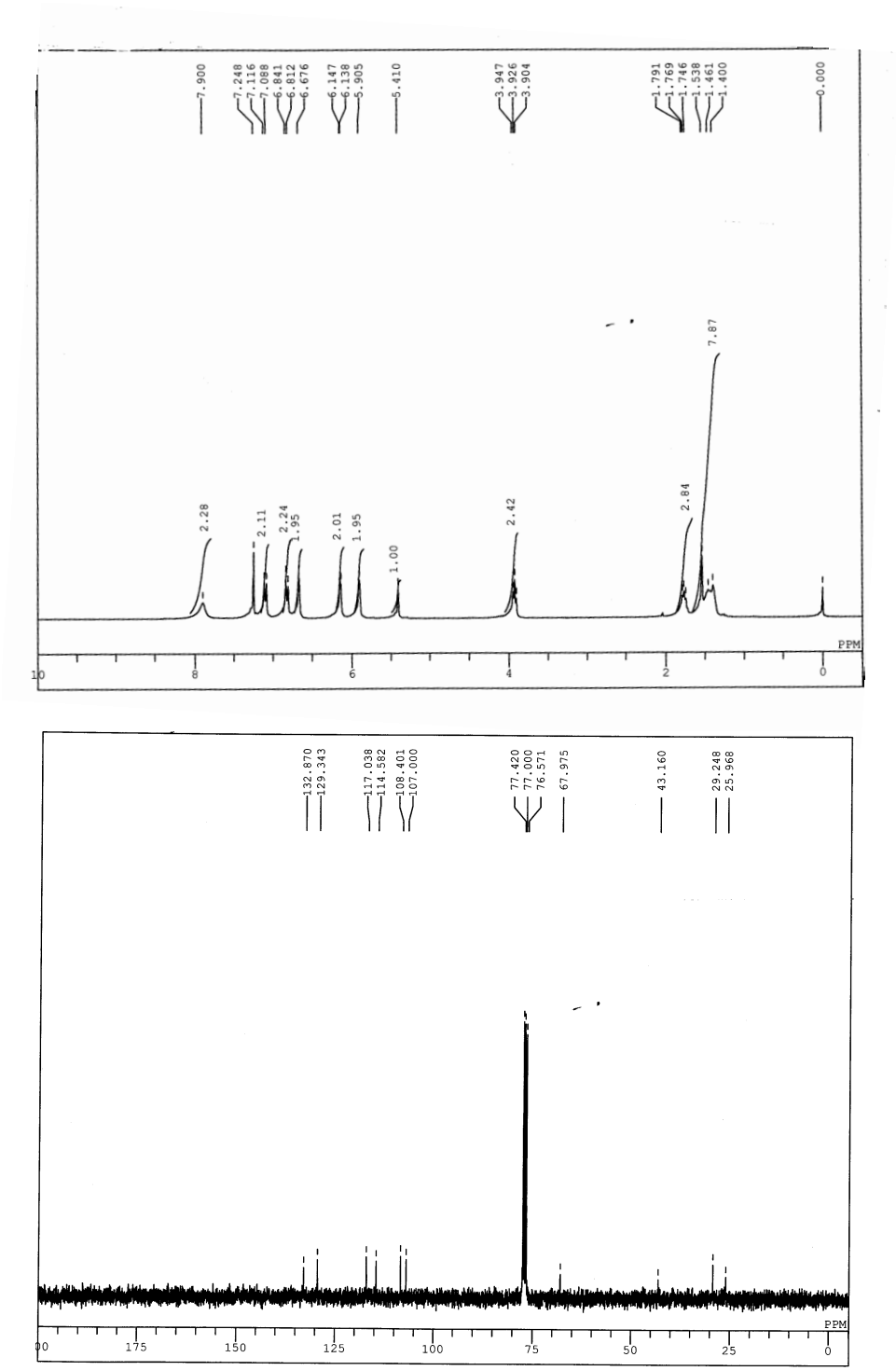

Fig. S27 ^{1}H (top) and ^{13}C NMR (bottom) spectra of **L7** in $CDCl_3$.

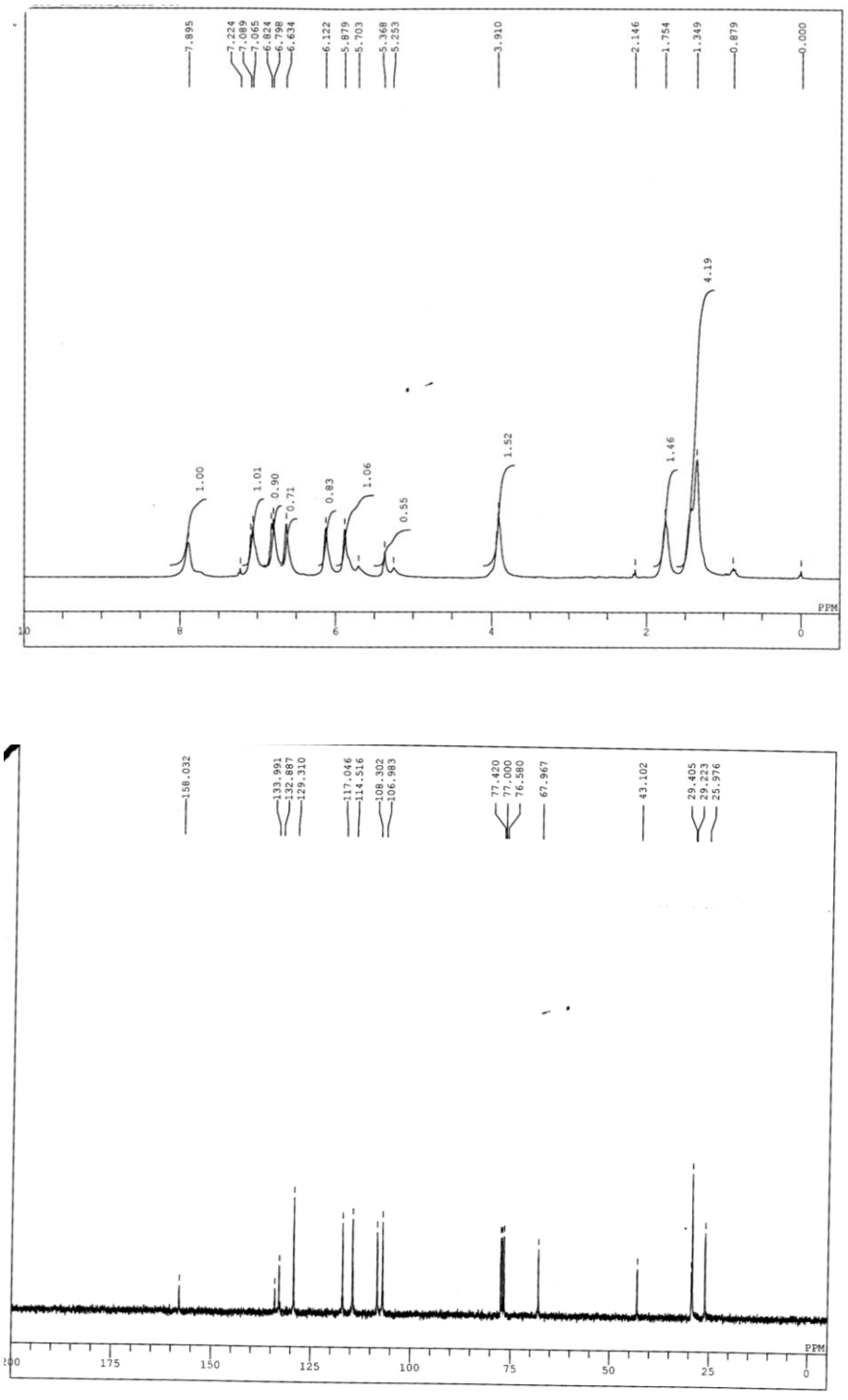

Fig. S28 ^{1}H (top) and ^{13}C NMR (bottom) spectra of **L8** in $CDCl_3$.

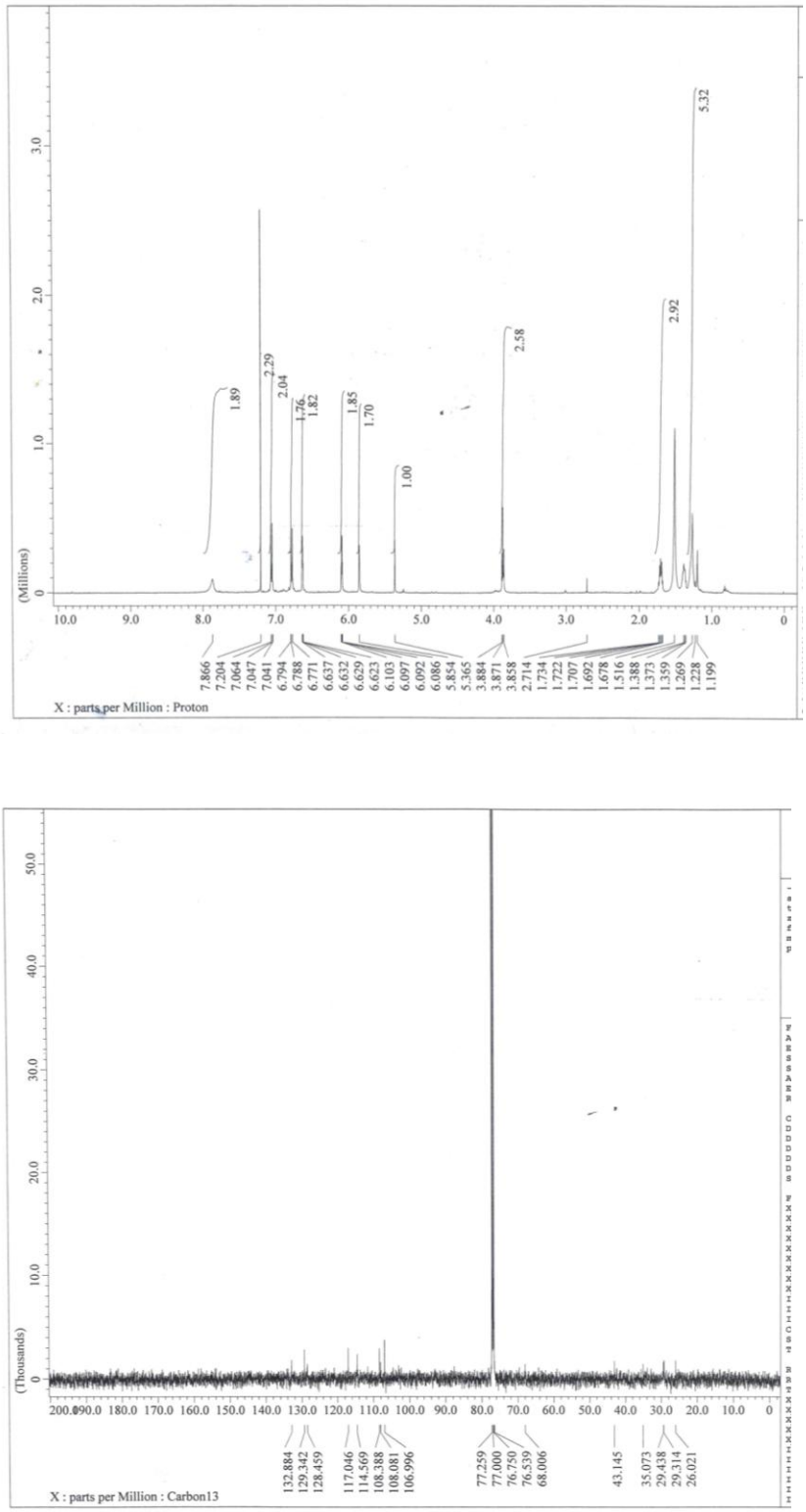

Fig. S29 ^{1}H (top) and ^{13}C NMR (bottom) spectra of **L9** in $CDCl_3$.

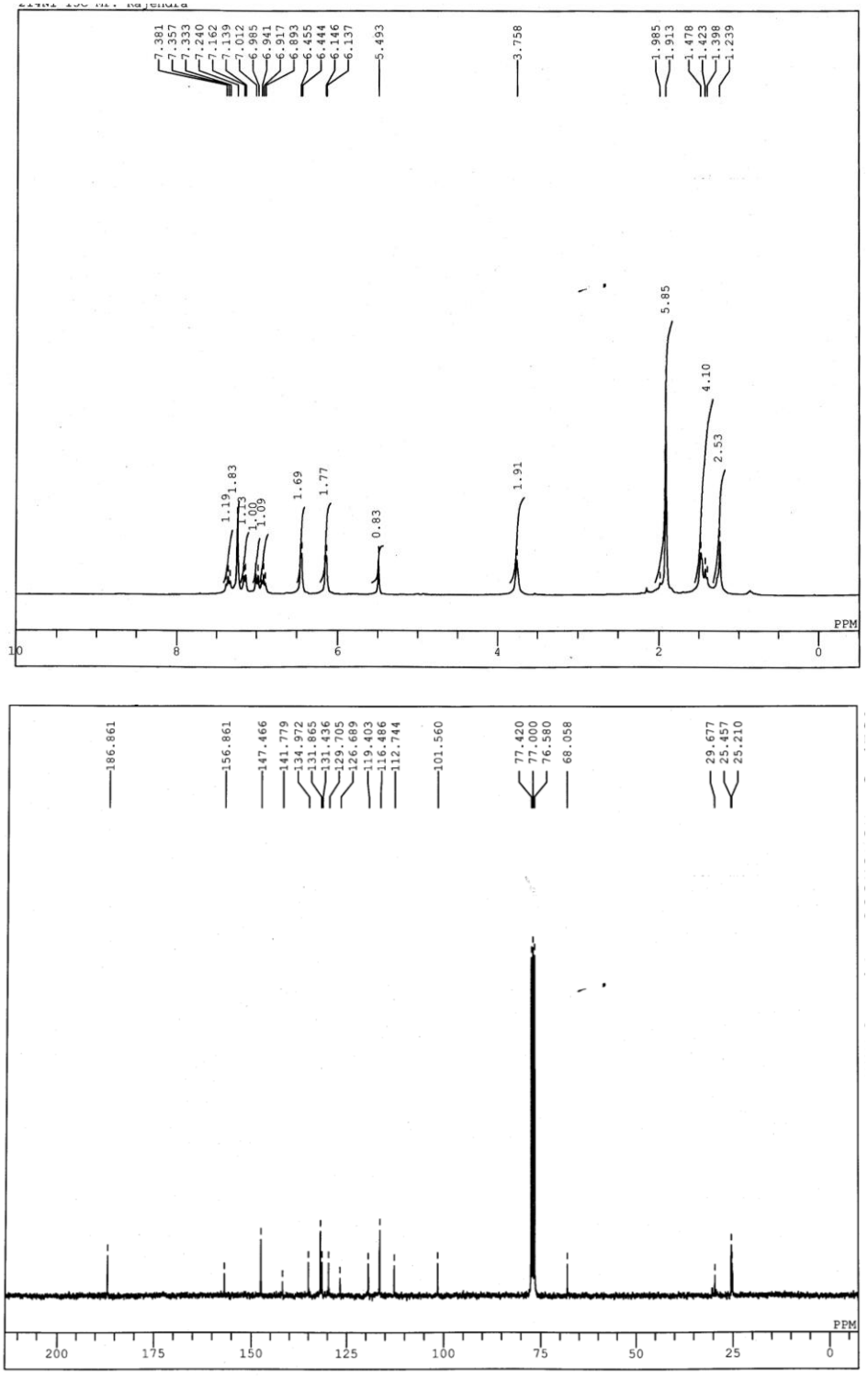

Fig. S30 ^{1}H (top) and ^{13}C NMR (bottom) spectra of **3″**in $CDCl_3$.

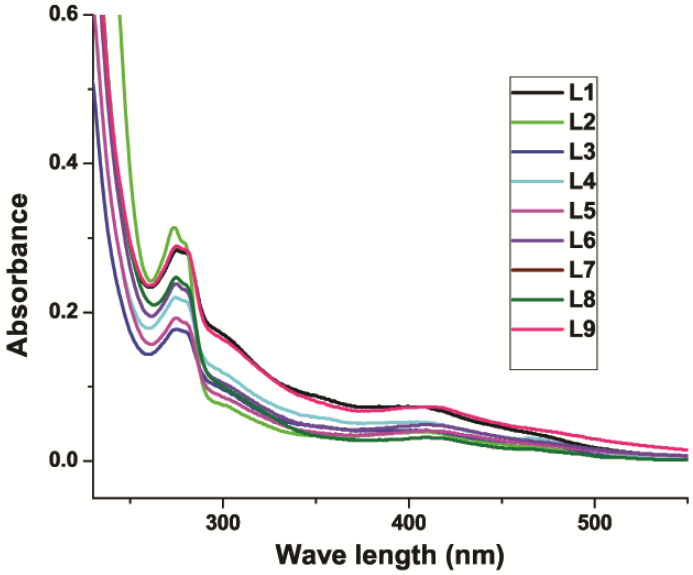

Fig. S31 UV/vis spectra of **L1–L9** in DCM (*c*, 10 μM) at room temperature.

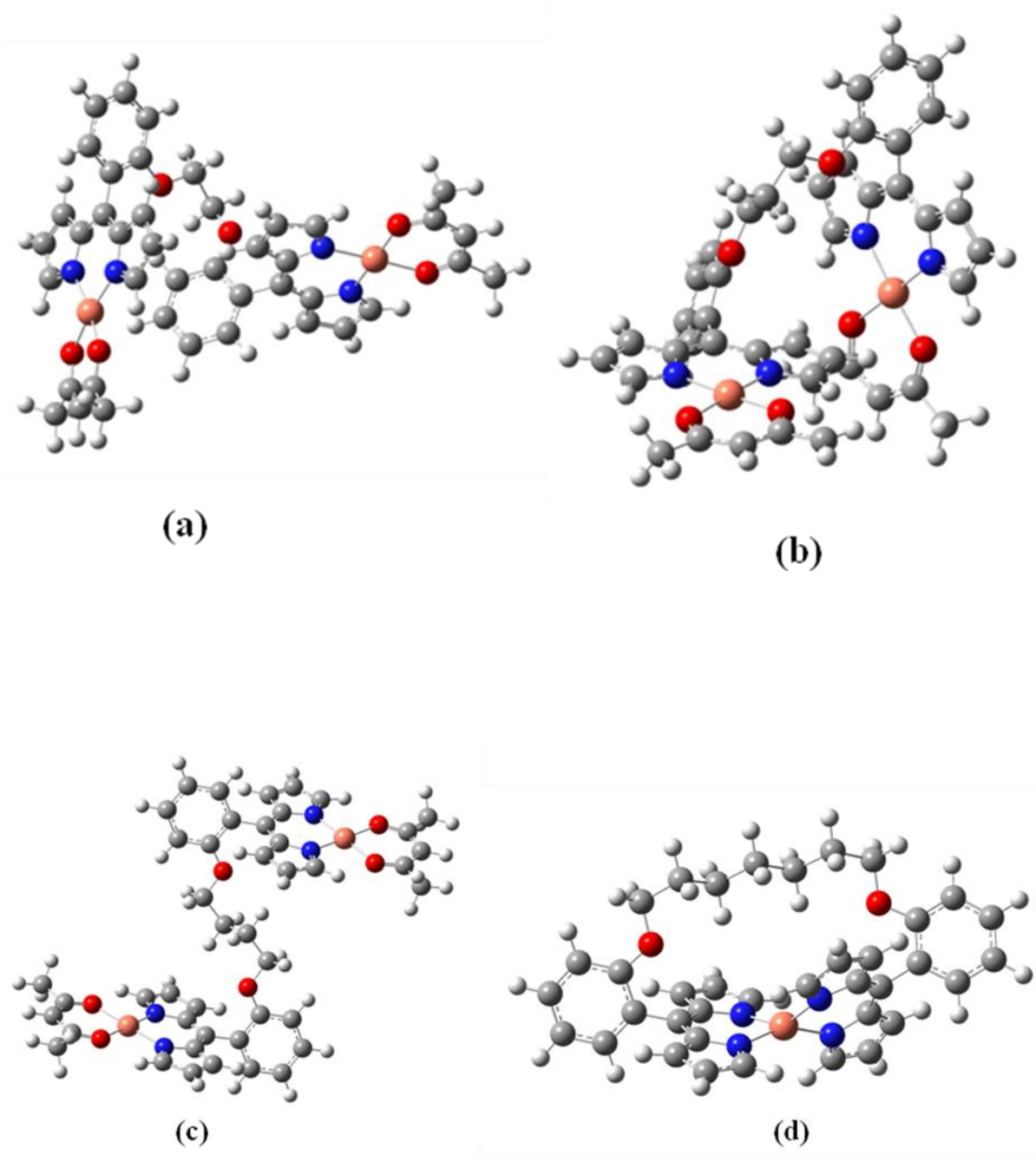

Fig. S32 DFT optimised structures of complex **1** (a), **2** (b), **3** (c) and **6** (d).

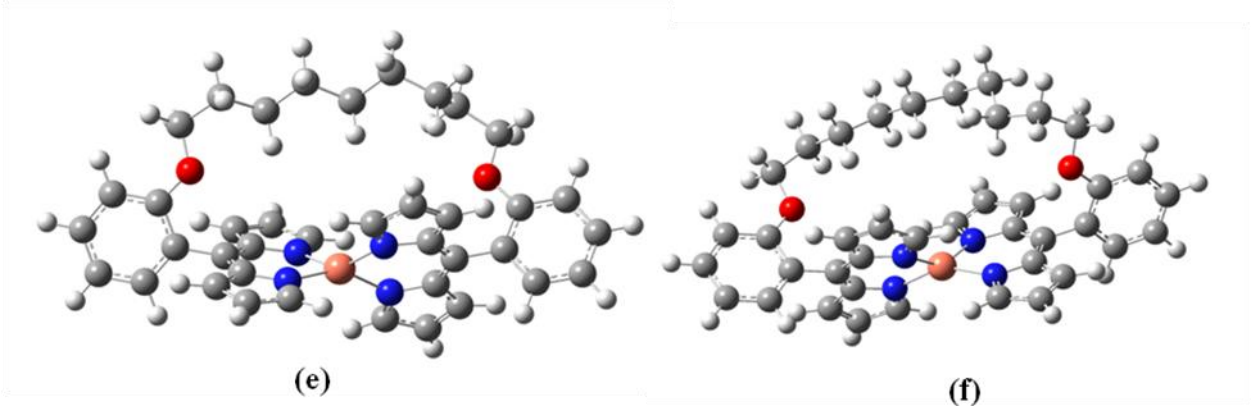

Fig. S33 DFT optimised structures of complex **8** (e) and **9** (f).

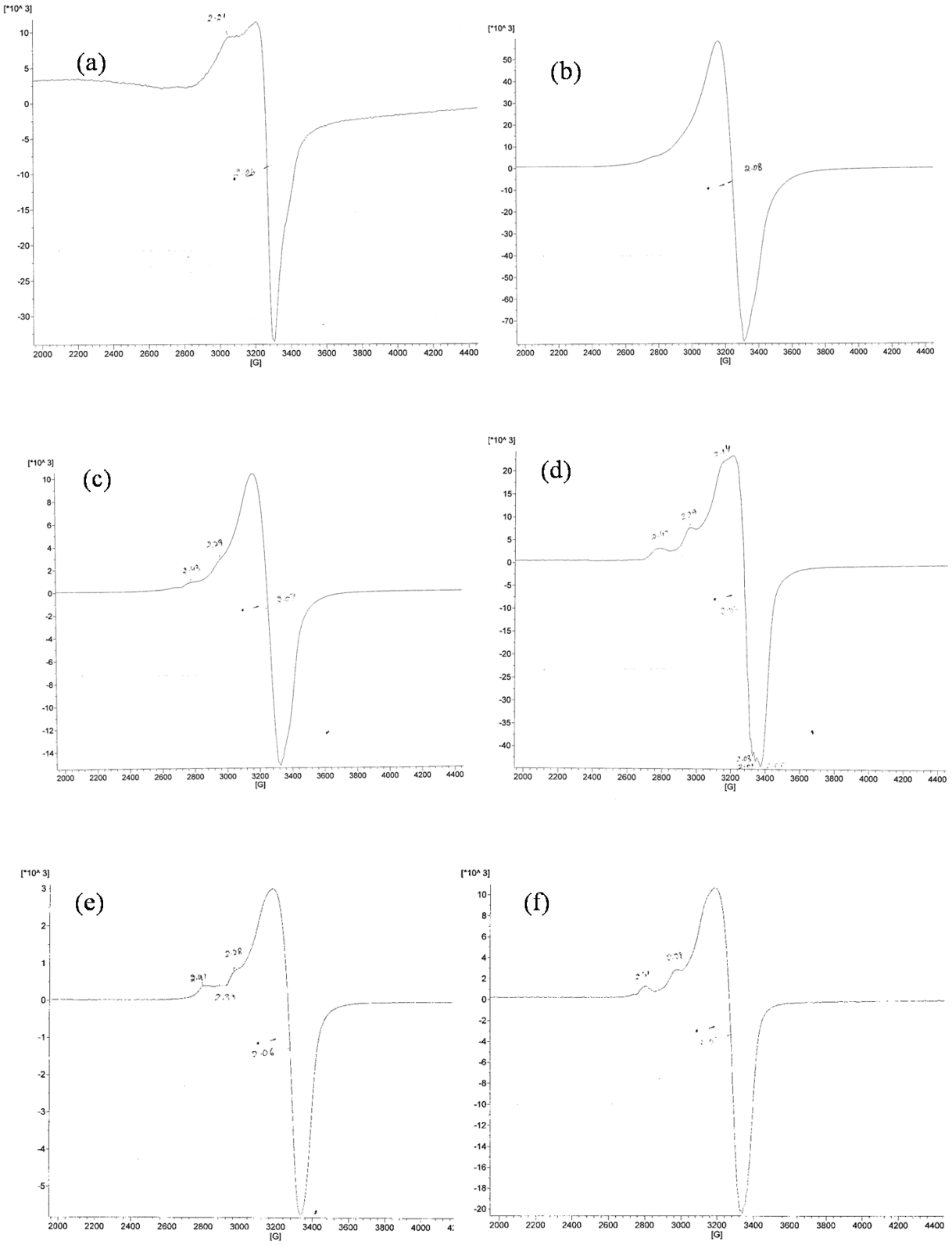

Fig. S34 EPR spectra of Complex **1**(a), **2**(b), **3**(c), **4**(d), 7(e) and 8(f) at liquid nitrogen temperature.

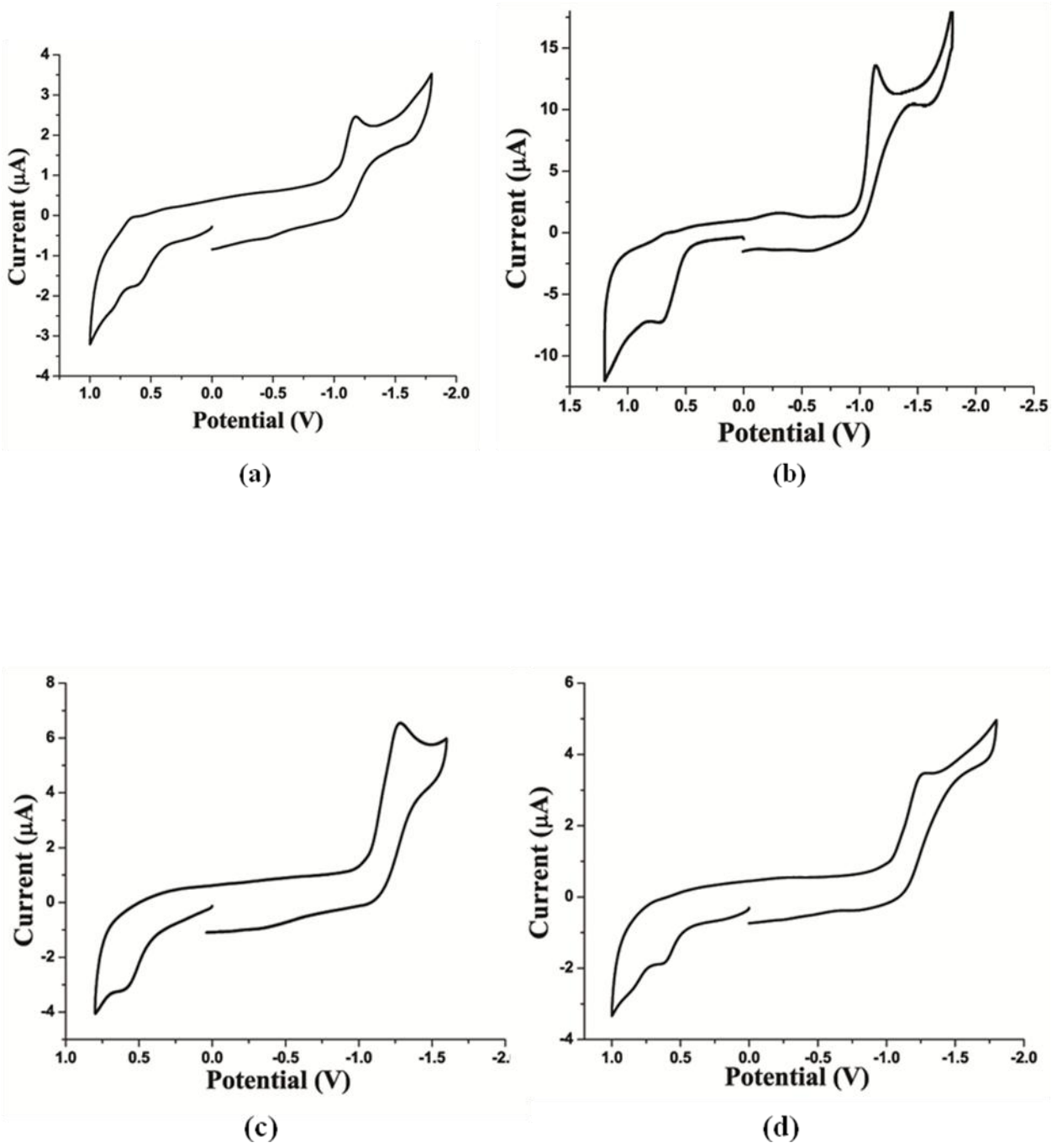

Fig. S35 Cyclic voltammogram of Complex **1** (a), **2** (b), **3** (c) and **4** (b) in CH_3CN (*c*, 100 μM), at room temperature.

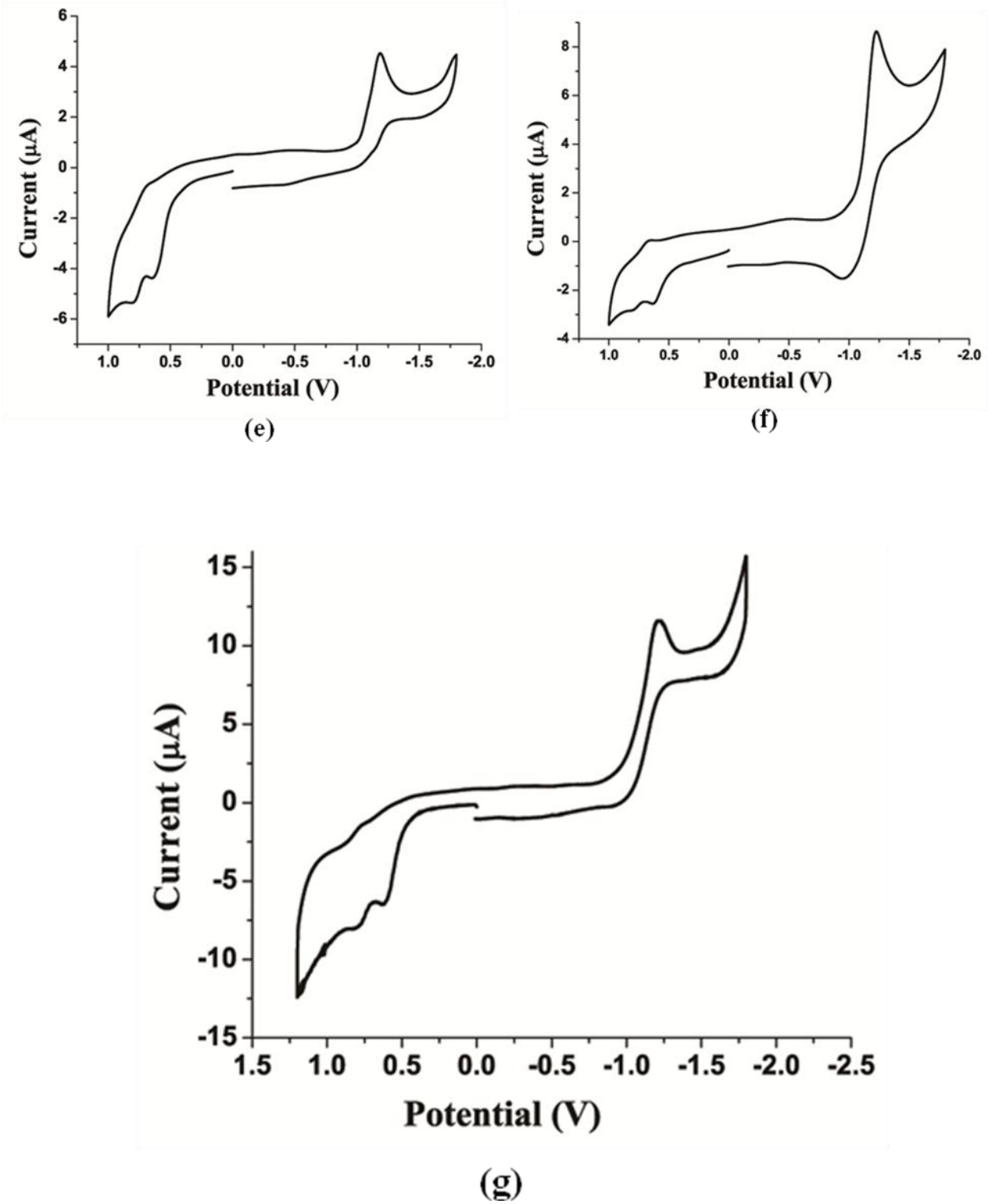

Fig. S36 Cyclic voltammogram of Complex **7** (e), **8** (f) and **9** (g) in CH_3CN (*c*, 100 μM), at room temperature.

Chronocoulometry

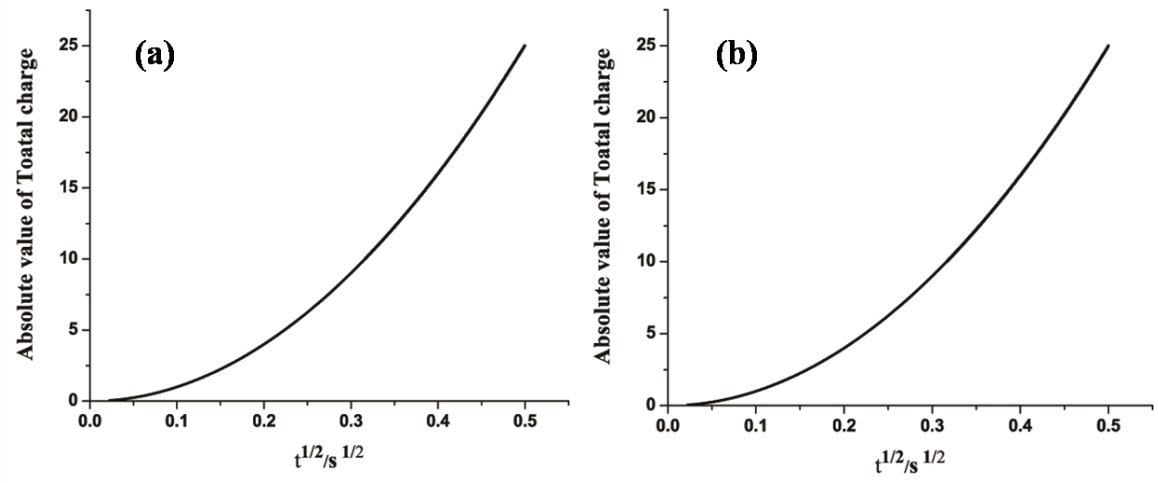

Fig. S37 Q|-$t^{1/2}$ plots of the oxidation process (a) and the reduction process (b) in the cyclic-voltammogram of **5**.

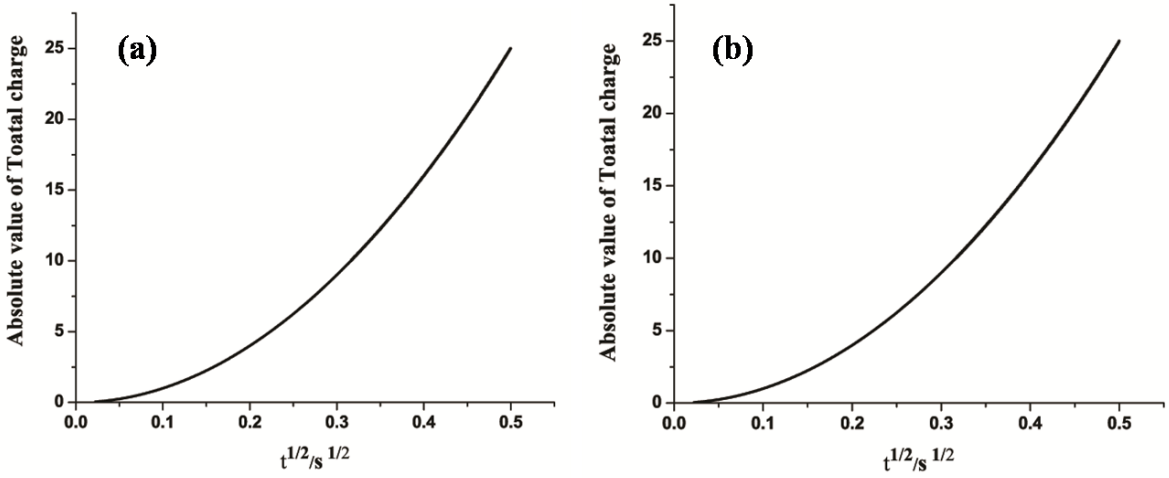

Fig. S38 Q|-$t^{1/2}$ plots of the oxidation process (a) and the reduction process (b) in the cycli-cvoltammogram of **6**.

Fig. 38–39 shows the $|Q|\text{-}^{t1/2}$ plots, for compound **5** and **6** respectively, where Q is the total charge and t is the elapsed time. Apart from the beginning of the polarization, where charging of the electric double layer plays a chief role, the $|Q|\text{-}t^{1/2}$ plot shows a linear relationship. Therefore, both the oxidation and reduction processes are diffusion-controlled. In this scenario, eq (1) may be applicable.

$Q = 2nFACD\pi 1/2t^{1/2}$ ……. (1)

Where n is the number of electrons involved in the redox reaction, F is the Faraday constant, A is the electrode area, C is the concentration, and D is the diffusion coefficient of the analyte. All factors are common for the oxidation and reduction for **5** and **6** except for n; hence, the slope of the $|Q|\text{-}t^{1/2}$ plot is proportional to n. For compound **5** the slopes are 7.39×10^{-6} and 7.38×10^{-6} for oxidation and reduction, respectively, where as for compound **6** slopes are 7.38×10^{-6} and 7.39×10^{-6} for oxidation and reduction, respectively indicating a ratio of 1:1 for n.

Table S1: Selected bond lengths (Å) and angles (˚) for complexes **1**–**5** through DFT calculations.

Bond length (Å)	**1**	**2**	**3**	**4**	**5**
Cu–N1	2.000	1.990	1.997	1.989	1.997
Cu–N2	1.996	1.988	1.995	1.988	1.996
Cu1–O1	1.992	1.983	1.990	1.981	1.989
Cu1–O2	1.997	1.960	1.989	1.954	1.990
Bond Angle (˚)	**1**	**2**	**3**	**4**	**5**
N1–Cu1–N2	90.83	90.93	90.50	90.87	90.57
O1–Cu1–O2	89.86	89.98	89.47	90.06	89.44
N2–Cu1–O1	90.53	89.76	90.04	89.73	90.03
N1–Cu1–O2	90.21	89.47	89.98	89.52	89.96

Table S2: Selected bond lengths (Å) and angles (˚) for **6**–**7** and **9** through DFT calculations.

	6 (XRD)	**6** (DFT)	**8** (XRD)	**8** (DFT)	**9** (XRD)	**9** (DFT)
Cu–N1	1.938	1.991	1.954	2.001	1.954	2.006
Cu–N2	1.969	2.009	1.943	1.996	1.945	1.994
Cu–N3	1.939	1.989	1.957	2.006	1.931	1.991
Cu–N4	1.964	2.010	1.955	1.993	1.939	2.004
Bond Angle (˚)	**6** (XRD)	**6** (DFT)	**8** (XRD)	**8** (DFT)	**9** (XRD)	**9** (DFT)
N1–Cu1–N2	92.5	91.09	92.2	91.16	91.4	91.08
N1–Cu1–N4	151.6	152.20	148.0	149.18	144.1	149.88
N2–Cu1–N3	137.0	142.87	145.2	145.20	149.0	149.22
N3–Cu1–N4	92.6	90.67	91.8	91.01	92.5	91.05

Table S3. EPR spectral data for **1**–**9**.

	1	**2**	**3**	**4**	**5**	**6**	**7**	**8**	**9**
$\mathbf{g}_{\parallel}$	2.24	2.24	2.23	2.24	2.25	2.30	2.28	2.27	2.27
$\mathbf{g}_{\perp}$	2.06	2.08	2.07	2.05	2.07	2.06	2.06	2.06	2.06
$\mathbf{A}_{\parallel \times 10^{-4}}$ (cm^{-1})	177	179	177	172	172	124	122	125	124
$\mathbf{g}_{\parallel}/\mathbf{A}_{\parallel}$ (cm^{-1})	127	125	126	130	130	185	186	181	183